APEM
journal

Advances in Production Engineering & Management

Advances in Production Engineering & Management

Identification Statement

APEM Editorial

Advances in Production Engineering & Management

Contents

Scope and topics

Advances in Production Engineering & Management (*APEM journal*) is an interdisciplinary refereed international academic journal published quarterly by the *Production Engineering Institute* at the *University of Maribor*. The main goal of the *APEM journal* is to present original, high quality, theoretical and application-oriented research developments in all areas of production engineering and production management to a broad audience of academics and practitioners. In order to bridge the gap between theory and practice, applications based on advanced theory and case studies are particularly welcome. For theoretical papers, their originality and research contributions are the main factors in the evaluation process. General approaches, formalisms, algorithms or techniques should be illustrated with significant applications that demonstrate their applicability to real-world problems. Although the *APEM journal* main goal is to publish original research papers, review articles and professional papers are occasionally published.

Fields of interest include, but are not limited to:

Additive Manufacturing Processes	Machine Tools
Advanced Production Technologies	Machining Systems
Artificial Intelligence	Manufacturing Systems
Assembly Systems	Mechanical Engineering
Automation	Mechatronics
Cutting and Forming Processes	Metrology
Decision Support Systems	Modelling and Simulation
Discrete Systems and Methodology	Numerical Techniques
e-Manufacturing	Operations Research
Fuzzy Systems	Operations Planning, Scheduling and Control
Human Factor Engineering, Ergonomics	Optimisation Techniques
Industrial Engineering	Project Management
Industrial Processes	Quality Management
Industrial Robotics	Queuing Systems
Intelligent Systems	Risk and Uncertainty
Inventory Management	Self-Organizing Systems
Joining Processes	Statistical Methods
Knowledge Management	Supply Chain Management
Logistics	Virtual Reality

Artificial neural network modeling for surface roughness prediction in cylindrical grinding of Al-SiC$_p$ metal matrix composites and ANOVA analysis

Chandrasekaran, M.[a,*], **Devarasiddappa, D.**[b]

[a]Mechanical Engineering Department, North Eastern Regional Institute of Science and Technology, Nirjuli, India
[b]Automobile Engineering Department, Rajiv Gandhi Government Polytechnic, Itanagar, India

A B S T R A C T

In the present work, surface roughness prediction model in cylindrical grinding of LM25/SiC/4$_p$ metal matrix composites (MMC) was developed using artificial neural network (ANN) methodology. The independent input machining parameters considered in the modeling were wheel velocity, feed, work piece velocity and depth of cut. The neural network architecture 4-12-1 with logsig transfer function was found optimum with 94.20 % model accuracy. The analysis of variance (ANOVA) was carried to study influence of the machining parameters on surface roughness. The study revealed higher *F*-ratio for wheel velocity and it found to be the most influencing parameter in prediction of surface roughness. The percentage of contribution for wheel velocity was 32.47 %, feed was 26.50 % and work piece velocity was 25.08 %. The depth of cut was found to have least effect on surface roughness with 13.22 % contribution. The independent and combined effect of process parameters on predicted value of surface roughness was studied using two-dimensional graphs and surface plots. The study showed that surface roughness increases as feed increases while it decreases with increase in wheel velocity. It was also observed that minimum surface finish could be obtained at high wheel and work piece velocities, and low feed and depth of cut.

1. Introduction

Metal matrix composites (MMC) having aluminium (Al) in the matrix phase and silicon carbide particles (SiC$_p$) in reinforcement phase, i.e. Al-SiC$_p$ type MMC, have gained popularity in the recent past. In this competitive age, manufacturing industries strive to produce superior quality products at reasonable price. This is possible by achieving higher productivity while performing machining at optimum combinations of process variables. The low weight and high strength MMC are found suitable for variety of components demanding high performance, especially in the automotive, aerospace, military, and medical applications [1]. The MMC provide advantages of higher specific strength and modulus over monolithic metals (steels and aluminium). Though the MMC can be produced to net-near shape, subsequent machining is found essential to bring them to the desired shape and size with proper surface integrity [2]. This is achieved by either of the machining processes viz. turning, milling or grinding. However, due to the hard and abrasive reinforcement used, MMC exhibit poor machinability resulting in accelerated tool wear and in-

creased manufacturing cost. Thus, higher machining cost has remained a major concern which has impeded significant use of MMC components [3, 4].

Surface roughness (R_a) is one of the main attributes of a machined component that characterizes surface topography. It is evidently influenced by cutting parameters, work-tool material, tool geometry and statistical variation during machining. Surface roughness predominantly describes the quality of finish and plays a crucial role in various engineering applications. Reasonable surface finish is always desirable to improve tribological aspects and aesthetic appearance where as excessive surface finish involves higher machining cost. Surface finish of a machined component is defined as the degree of smoothness of surface as a result of roughness, waviness and flaws generated due to machining. Among various methods available, center line average (CLA) method is most commonly used for the measurement of surface roughness. In this method, surface roughness is measured as the average deviation from the nominal surface and mathematically expressed as in Eq. 1.

$$R_a = \frac{1}{L} \int_0^L |Y(x)|\, dx \qquad (1)$$

where, R_a is arithmetic average deviation from the mean line, L is sampling length, and Y is ordinate of the roughness profile.

Modeling of surface roughness prediction has been attempted using multiple regression analysis, response surface methodology (RSM), fuzzy logic (FL), and artificial neural network (ANN). The study of influence of cutting parameters on surface roughness in MMC machining has been the focused area in academia. The soft computing techniques viz. ANN and FL found effective to model machining processes which are complex in nature.

Among the gamut of soft computing techniques, ANN and FL are the two important methods effectively applied for modelling and optimization of machining processes. Number of researchers has used these tools to develop predictive models in various machining processes. In the area of machining, ANN modelling techniques have been commonly used for the prediction of surface roughness, cutting forces, tool wear, tool life and dimensional deviation [5]. Recently, gravitational search algorithm (GSA) was applied for modelling of a turning process with multiple responses (main cutting force, surface roughness and tool life) by Hrelja et al. [6]. The coefficients of the polynomial model for each of the responses were optimized iteratively using PSO algorithm. The optimized model for cutting force was reported to be most accurate with 1.75 % average error (maximum error: 6.3 %) followed by prediction model for surface roughness (average error: 5.85 %, maximum error: 43 %) and tool life (average error: 24.5 %, maximum error: 60 %). The higher values of error were attributed to fewer datasets used in the knowledge base during the learning phase. The ANN and FL techniques were used to develop knowledge based system for prediction of surface roughness in turning process [7]. The knowledge based system consisted of a ANN module which is used to generate large data set to form if-then rules of the fuzzy model. A methodology that requires small size data set for ANN modeling is presented by Kohli and Dixit [8]. Risbood et al. [9] developed a multilayer perceptron (MLP) model for prediction of multiple responses (surface roughness and dimensional deviation) in wet turning of steel with HSS tool with four input parameters. The error in surface roughness prediction was reported nearly 20 %.

Routara et al. [10] applied RMS to develop the second order mathematical models for surface roughness prediction. The models were further optimized by genetic algorithm (GA) to find the optimum cutting parameters.

Sonar et al. [11] used radial basis function neural network (RBFN) for prediction of surface roughness in turning process with same accuracy in shorter computational time. Contrarily, the surface roughness prediction using neural network (NN) model was found less accurate than FL and regression models in hard turning of AISI 4140 steel [12]. The RBFN found more accurate than multi variable regression analysis in the prediction of thrust force and surface roughness in drilling of carbon fiber reinforced polymer (CFRP) composite materials [13]. The NN and FL

models reported to predict multiple responses, i.e. material removal rate, tool wear and radial over cut with agreeable accuracy (prediction error 4.94-16.22 %) in electrical discharge machining of AISI D2 steel [14]. Optimization of machining parameters using ANN was found effective in comparison with analysis of variance (ANOVA) by Muthukrishan and Davim [15] in turning of Al-SiC$_p$ MMC. The influence of machining parameters on surface roughness in drilling [16] and in end milling [17] of Al-SiC$_p$ MMC has been studied using RSM. The surface roughness is predominantly influenced by feed rate and cutting speed. The depth of cut reported to have least effect.

Thiagarajan et al. [18] have carried out experimental investigation of surface integrity during cylindrical grinding of LM25/SiC$_p$ MMC and reported that wheel velocity, job velocity and feed are the main influencing factors. The NN prediction models based on two different training algorithms viz., scaled conjugate gradient (SCG) and Levenberg-Marquardt (LM) compared with multiple regression models in turning of AISI 1040 steel [19]. Both the NN models found better in prediction than regression model. A similar work was carried out by Pare et al. [20] for cutting force prediction in turning of titanium alloy. The ANN model prediction found superior to RSM. Edwin Raja Dhas and Somasundaram [21] found ANN technique and fuzzy logic to accurately predict weld residual stress. Devarasiddappa et al. [22] developed ANN model for predicting the surface roughness in end milling of Al-SiC$_p$ MMC using small set of experimental data sets. The predictive performance of the model was found highly encouraging with average error of 0.31 % as against 0.53 % for the RSM published result.

Number of researchers has carried out the experimental study and modeling of different machining processes by employing both conventional and soft computing based methodology. Recently, ANN is used as popular and promising technique for prediction surface roughness in machining process. Though, a large number of research publications are available on MMC machining, few publications are available in MMC grinding. In this paper, development of ANN based model for prediction of surface roughness during cylindrical grinding of Al-SiC$_p$ MMC has been attempted. The various machining parameters and their influences on job surface roughness were studied. The development of ANN predictive model and analysis of process parameters is detailed out in subsequent sections.

2. Development of surface roughness prediction model

In order to improve machining process, surface roughness prediction model is developed. There are four common techniques for the development of a prediction model: 1) multiple regressions, 2) physics based modeling, 3) ANN, and 4) FL based models. ANN is one of the most widely used artificial intelligent techniques and has been successfully employed by researchers. It has ability to learn the mapping between a set of input and output values.

2.1 Artificial neural network modeling

The ANN is a data processing system consisting of a large number of simple and highly interconnected processing elements resembling biological neural system. It can be effectively used to determine the input-output relationship of a complex process and is considered as a tool in nonlinear statistical data modeling. A multilayer NN that works on back propagation learning algorithm was used in the present work. The ANN model was trained initially using experimental data so as to predict response variable(s) for unknown input datasets within reasonable accuracy.

In the present work, ANN model was developed for predicting surface roughness in cylindrical grinding of Al-SiC$_p$ MMC (i.e., LM25/SiC/4$_p$) using vitrified-bonded white aluminium oxide grinding wheel. The independent input machining parameters considered were (a) cutting speed of the grinding wheel, V_s (m/min), (b) cutting speed of the work piece, V_w (m/min), (c) feed, f (m/min), and (d) depth of cut, d (μm). For training the neural network, real life datasets obtained through machining experimentation from experimental result of Thiagarajan et al. [19] were used. The four process parameters at three different levels were considered for experimentation. The level of the parameters considered is given in Table 1.

Table 1 Levels of parameters used for experimentation

Parameters	Level 1	Level 2	Level 3
V_s (m/min)	1414	2026	2639
V_w (m/min)	6.11	12.72	26.72
f (m/min)	0.06	0.09	0.17
d (µm)	10	20	30

2.2 Network architecture and training

A typical multilayer ANN model consists of input, hidden and output layers. The ANN architecture consisting of an input layer with four neurons each representing one input variable, one hidden layer (12 neurons) and an output layer with one neuron having purelin processing function was employed in the present work. The model was trained using 20 experimental datasets given in Table 2 including corner datasets of each variable. The five datasets given in Table 3 were used for testing the model during training. The source code was written in MATLAB version 7.8.

Table 2 Experimental datasets used for ANN model training

Sl. No	V_s (m/min)	V_w (m/min)	f (m/min)	d (µm)	R_a (µm)
1	1414	6.11	0.06	10	0.40
2	1414	6.11	0.06	30	0.58
3	1414	6.11	0.17	10	0.67
4	1414	12.72	0.06	10	0.34
5	1414	12.72	0.09	30	0.72
6	1414	12.72	0.17	20	0.78
7	1414	12.72	0.17	30	0.86
8	1414	26.72	0.06	10	0.25
9	2026	6.11	0.09	10	0.46
10	2026	6.11	0.17	30	0.80
11	2026	12.72	0.09	20	0.43
12	2026	26.72	0.06	10	0.19
13	2026	26.72	0.09	20	0.34
14	2026	26.72	0.17	30	0.42
15	2639	6.11	0.09	20	0.43
16	2639	6.11	0.17	30	0.52
17	2639	12.72	0.06	30	0.29
18	2639	26.72	0.06	10	0.18
19	2639	26.72	0.17	10	0.19
20	2639	26.72	0.17	30	0.38

The Fig. 1 depicts the two layer feed forward NN used in this work. The input layer consists of 4 neurons as wheel speed, workpiece speed, feed and depth of cut being the control parameters. The output layer consists of one neuron having purelin processing function. The NN training was performed for desired error goal of 0.0001 by varying hidden layer neurons from 5-20 for two different transfer functions – tansig and logsig.

The number of neurons in the hidden layer plays a vital role in deciding the optimal architecture of the model. If less number of neurons are taken, the network may not be able learn the input-output relationship properly and the error in prediction will be higher. Increasing the number of neurons in the hidden layer gives more flexibility to the network because the network has more parameters it can optimize and hence learning can be more accurate.

Table 3 Testing datasets used for ANN model development

Sl. No	V_s (m/min)	V_w (m/min)	F (m/min)	d (µm)	R_a (µm)
1	1414	6.11	0.09	20	0.69
2	1414	6.11	0.17	20	0.80
3	1414	12.72	0.06	30	0.48
4	1414	26.72	0.09	10	0.33
5	2639	26.72	0.06	30	0.23
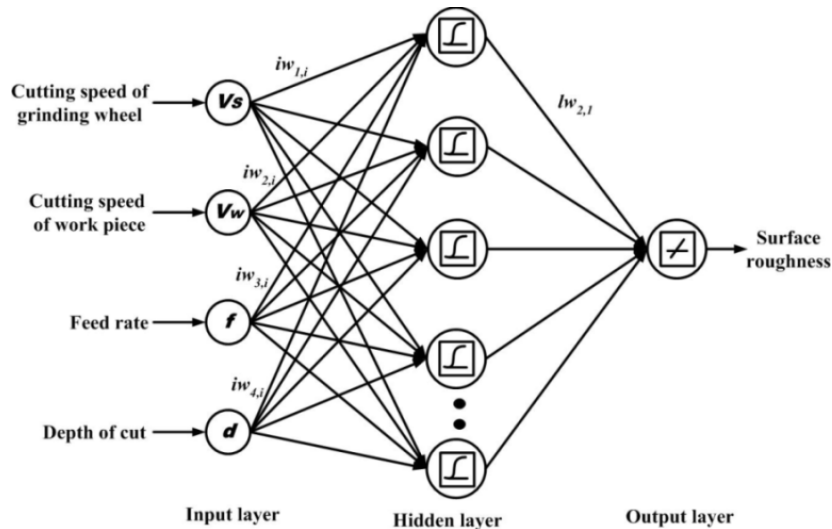
Fig. 1 Typical two layer NN architecture used

However, if the hidden layer neurons are too large, it might cause the problem to be under-characterized since the network has to optimize more parameters than there are data vectors to constrain these parameters. Thus the generalization capability of the network and hence its performance is compromised with large number of neurons in the hidden layer. The selection of suitable transfer function is also equally important. The transfer function is used to calculate the output from the input parameters. In the present work, the log sigmoid (logsig) transfer function found suitable for the hidden layer. The Eq. 2 and Eq. 3 represent logsig and purelin transfer functions, respectively,

$$a = logsig\ (n) = \frac{1}{1 + e^{-n}} \tag{2}$$

$$a = purelin\ (n) = n \tag{3}$$

where *n* is net weighted input to the neuron.

The neural network was trained with different number of neurons (varying from five to twenty) and different transfer functions in the hidden layer. The maximum number of epochs allowed in each run is 25000. The code was run five times at each network topology with different initial random weights. The network configurations giving average percentage error in training and testing data set within 15 % were recorded. A properly trained NN gives nearly equal training and testing error. A network having smaller training error exhibits poor generalization capability and thus predicts poorly for new datasets. The detail of training and testing error for different network topology is presented in Table 4 and its graphical representation is depicted in Fig. 2.

Table 4 Network training result for different architectures

Sl. No.	NN architecture	Average percentage error		Effective error (%)
		Training	Testing	
1	4-6-1 (tansig)	8.66	12.12	3.46
2	4-15-1 (logsig)	11.93	8.53	3.40
3	4-17-1 (tansig)	11.32	14.59	3.27
4	4-18-1 (logsig)	11.79	14.38	2.59
5	4-11-1 (tansig)	3.83	5.73	1.90
6	4-12-1 (logsig)	10.55	9.35	1.20
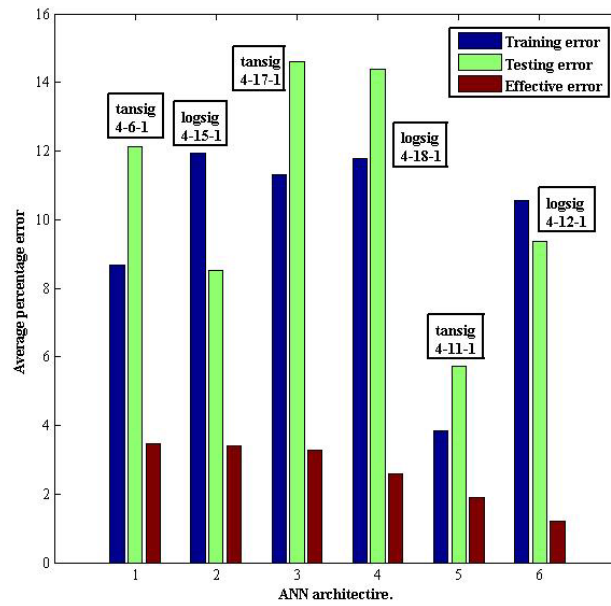
Fig. 2 Selection of optimal NN architecture

The NN was trained using trainbr (Bayesian regulation back propagation) training function which uses Bayesian regularization. The training datasets of the converged network are given in Table 2. The testing datasets of the converged network are presented in Table 3. The network was trained with a different data set (80 %) each time, which were randomly selected. The testing datasets (20 %) were also selected randomly. The network converged at 362nd iteration. The weights and biases as well as sum squared weights of converged network remains constant. The sum squared error (SSE) during testing recorded approximately 0.1311 and remained constant. The SSE during training was found to be 0.4269. The mean squared error in training and testing datasets of the converged NN model was found to be 0.0025 and 0.0031 respectively.

The optimum number of neurons and the selected transfer function that produce minimum effective error found as best network architecture. The ANN architecture 4-12-1 with logsig transfer function giving effective error of 1.20 % was found optimum in this work. At optimum network, weights and bias were saved and used to predict surface roughness for unknown datasets.

2.3 Network prediction performance

Accuracy of the NN predictive model was tested for 10 randomly selected experimental datasets. The model predicted R_a values were compared with experimental values and percentage error was calculated. The results are presented in Table 5.

The maximum and minimum percentage error recorded as 14.71 % and 0.0 %, respectively. The average percentage error (APE) and mean squared error (MSE) was computed using Eq. 4 and Eq. 5, respectively,

$$APE = \frac{1}{n}\sum_{i=1}^{n}\left(\frac{|t_i - y_i|}{t_i}\right) \times 100 \tag{4}$$

$$mse = \frac{1}{n}\sum_{i=1}^{n}(t_i - y_i)^2 \tag{5}$$

where t_i is target value for data set i, y_i is predicted value for data set i, and n is the total number of data sets.

Table 5 Validation result of neural network model

Sl. No.	Datasets used				R_a (μm)		Procentage error	Prediction accuracy
	V_s (m/min)	V_w (m/min)	f (m/min)	d (μm)	Exp.	ANN		
1	1414	6.11	0.06	20	0.54	0.51	5.56	94.44
2	1414	6.11	0.09	10	0.52	0.57	9.62	90.38
3	1414	6.11	0.17	30	0.88	0.89	1.14	98.86
4	1414	26.72	0.09	30	0.5	0.46	8.00	92.00
5	2026	12.72	0.06	20	0.34	0.31	8.82	91.18
6	2026	26.72	0.06	30	0.29	0.29	0.00	100.00
7	2026	26.72	0.09	30	0.34	0.39	14.71	85.29
8	2639	6.11	0.06	20	0.34	0.36	5.88	94.12
9	2639	12.72	0.17	30	0.52	0.51	1.92	98.08
10	2026	6.11	0.06	20	0.42	0.41	2.38	97.62
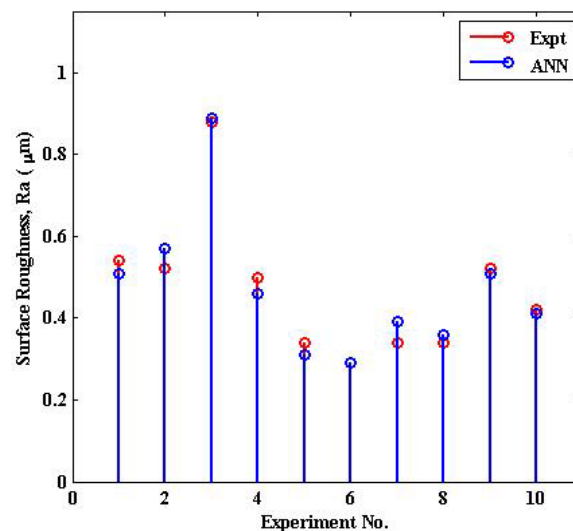
Fig. 3 Validation result of NN model

The average percentage error and MSE was found to be 5.80 % and 0.00091 respectively. The graphical representation of the NN prediction for validation data set is depicted in Fig. 3.

Model accuracy (MA) was computed as the average of individual accuracy on confirmation data set [23]. It is expressed by Eq. 6. The model accuracy of the developed model based on its predictive capability was found to be 94.20 %.

$$MA = \frac{1}{n}\sum_{i=1}^{n}\left(1 - \frac{|t_i - y_i|}{t_i}\right) \times 100 \tag{6}$$

3. Analysis of process parameters

The NN predicted surface roughness values were analysed to study the effect of process parameters. ANOVA technique was used to determine the significant control parameters affecting surface roughness.

3.1 Analysis of variance

ANOVA is a method of portioning variability into identifiable sources of variation and the associated degree of freedom in the model. Four control parameters were considered in the present study. Each factor affects the response to a varying degree. There were 3 levels (low, medium, and high) on four control parameters having 3^4 factorial designs of 81 experimental cutting conditions (datasets). The surface roughness for these datasets was predicted from the developed NN model.

ANOVA is used to decompose the total variability to quantify the effect machining parameters on surface roughness. The percentage contribution of machining parameters was estimated based on the sum of squares of responses. The grand total sum of squares (SS_{grand}) was evaluated using the Eq. 7.

$$SS_{grand} = \sum_{i=1}^{81} R_{ai}^2 \tag{7}$$

The SS_{grand} is decomposed into sum of squares due to mean (SS_{mean}) and total sum of squares (SS_{total}) using Eq. 8 and Eq. 9, respectively,

$$SS_{mean} = 81 \times R_{am}^2 \tag{8}$$

$$SS_{total} = \sum_{i=1}^{81} (R_{ai} - R_{am})^2 \tag{9}$$

where R_{am} is mean of responses. The sum of squares due to a factor is equal to its total squared deviation from the overall mean. In the present study, there were 27 experiments for each factor at each level. The sum of squares due to factor A (SS_A) was computed using the Eq. 10,

$$SS_A = 27(R_{aA1} - R_{am})^2 + 27(R_{aA2} - R_{am})^2 + 27(R_{aA3} - R_{am})^2 \tag{10}$$

where, R_{aA1}, R_{aA2}, and R_{aA3} are the mean of R_a at the level 1, 2, and 3 of the factor A, respectively. The relative importance of factor A influencing the surface roughness was computed as the percentage contribution (PC_A) using Eq. 11.

$$PC_A = \frac{SS_A}{SS_{total}} \times 100 \tag{11}$$

Similarly, the total sum of squares due to factor B (SS_B), C (SS_C) and D (SS_D) and their respective percentage contribution PC_B, PC_C, and PC_D were computed as detailed above. Table 6 shows the results of ANOVA for surface roughness. The degrees of freedom (DF), sum of squares (SS), mean of squares (MS), F-ratio and PC associated with each factor is also presented. This analysis was carried out at 5 % significance level, i.e. at 95 % confidence level.

The calculated values of the F-ratio showed high influence of the wheel velocity, feed and work piece velocity on surface roughness. The contributions of all the control parameters including error are presented pictorially in the pie chart shown in Fig. 4.

The cutting speed of the grinding wheel has the highest influence both in NN model as well as statistically on the surface roughness. Feed and cutting speed of work piece has almost equal influence on the surface roughness. However, the value of surface roughness is inversely proportional to work piece velocity but directly proportional to the feed. The error associated with the ANOVA analysis found minimum as 2.73 %.

Table 6 Result of ANOVA

Control factors	DF	SS	MS	F-ratio	PC
A: Wheel velocity	2	71.77	35.88	358.88	32.47
B: Job velocity	2	55.44	27.72	277.2	25.08
C: Feed	2	5858	29.29	292.9	26.50
D: Depth of cut	2	29.20	14.60	146.0	13.22
E: Error	72	6.03	0.1		2.73
Total	80	221.02			100.00
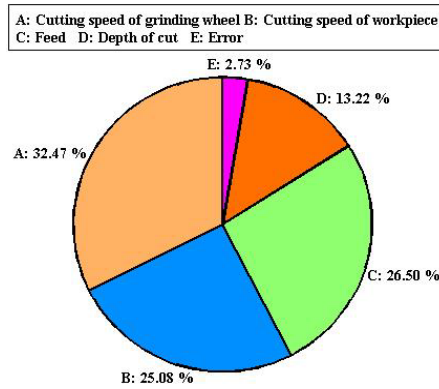
Fig 4 Contribution of control parameters

3.2 Study on influence of process parameters

The performance of the NN based predictive model for predicting the surface roughness was found very encouraging with 5.80 % average percentage error when compared with the experimental results. Based on model prediction, the influence of the process parameters on surface roughness was studied. The effect of these parameters was plotted graphically and is shown in Fig. 5a and Fig. 5b. The increase in wheel speed and workpiece speed improves the surface finish (i.e. surface roughness value reduces) of the job. The value of surface finish deteriorates as work feed increases. The surface finish improves at lower depth of cut as the cutting load lowers at low feed and low depth of cut.
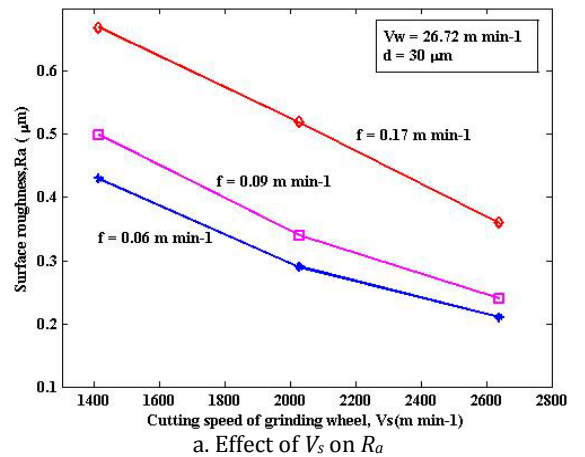
a. Effect of V_s on R_a
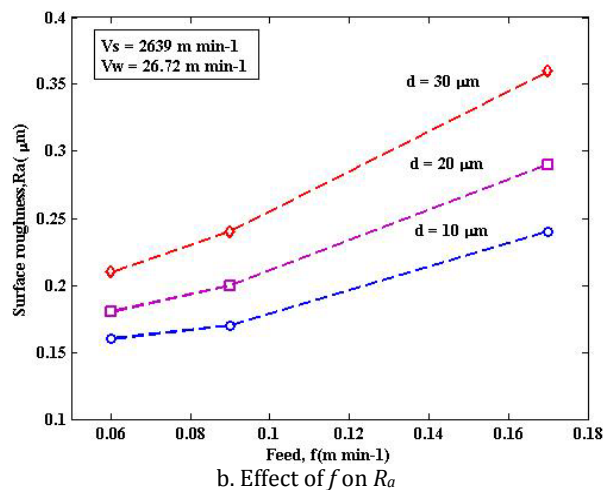
b. Effect of f on R_a

Fig 5 Effect of process parameters on surface roughness

a. Surface plot of R_a with f and V_s

b. Surface plot of R_a with d and f
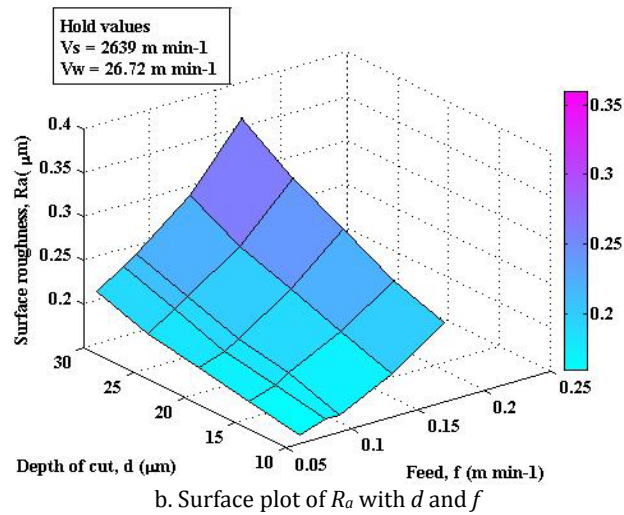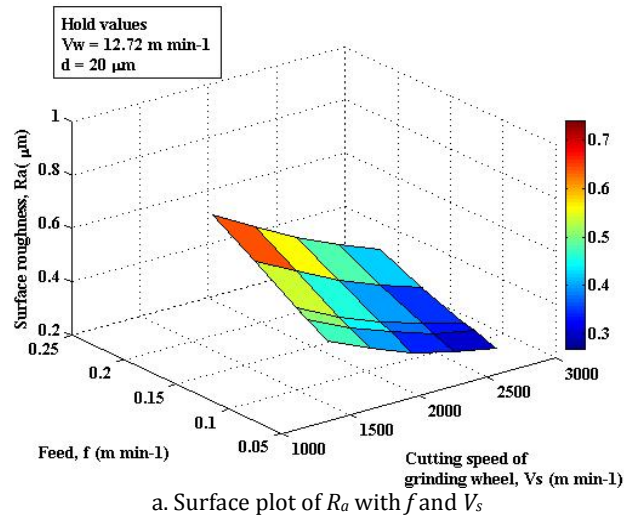
Fig. 6 Surface plots for combined effect of process parameters on R_a

The Fig. 6a shows the surface plot of surface roughness with feed and wheel velocity when work piece velocity and depth of cut are kept constant. The increase in wheel velocity reduces the surface roughness value. On the other hand, in case of feed, the value of surface roughness increases as feed increases. The plot shows the effect these parameters for the workpiece velocity of 12.72 m/min and depth of machining of 20 μm. The same effect was seen on work piece velocity and feed verses surface roughness. The minimum surface roughness was obtained at low depth of cut. The Fig. 6b depicts the surface plot of surface roughness with feed and depth of cut when wheel velocity and work piece velocity are held constant. The plot reveals that the minimum surface roughness value can be obtained at low feed and low depth of cut. With the combination of all parameters improved surface finish was obtained at high wheel velocity and work piece velocity. However, in case of feed and depth cut, the improved surface finish obtained at low feed and depth of cut due to reduced cutting load.

4. Conclusion

In the present work, the ANN model for prediction of surface roughness in cylindrical grinding of Al-SiC$_p$ MMC was developed. For NN modeling, the datasets were obtained from experimental result presented in [18]. The surface roughness value for different combination of process parameters was obtained and analyzed. The wheel velocity, work piece velocity, feed and depth of cut were considered as process parameters. The ANN architecture 4-12-1 with logsig transfer

function giving effective error of 1.20 % was found optimum in the present work. The predictive model was validated with confirmation datasets. Based on NN prediction model and analysis of the parameters, the following conclusions were drawn.

- The proposed neural network modeling was found easy and promising technique to develop predictive model for mapping input and output parameters. The developed model predicted surface roughness accurately for unseen data with 94.20 % model accuracy.
- The result of ANOVA showed highest *F*-ratio for wheel velocity and is the most significant influencing parameter for prediction of surface roughness. The percentage of contribution for wheel velocity was 32.47 %, feed was 26.50 %, and work piece velocity was 25.08 %. The depth of cut was found have least effect on surface roughness with 13.22 % contribution.
- The investigations on this study indicate that the process parameters wheel velocity, work piece velocity, feed and depth of cut are the primary influencing factors which affect the surface roughness of ground MMC component.
- The NN prediction revealed that better surface finish could be obtained at high wheel velocity and high work piece velocity. This is due to development of low grinding force at high speed of operation. The surface finish deteriorates at high feed and depth of cut as it increases the grinding load. The minimum surface finish was obtained with the combination of high wheel and workpiece velocity and low feed and depth of cut. The neural network predicted 0.16 μm being the minimum surface roughness at V_s = 2639 m/min, V_w = 26.72 m/min, f = 0.06 m/min and d = 10 μm.

The proposed methodology could be effectively employed for prediction of responses in variety of machining processes on different material combinations. The detailed ANOVA presented in this paper could be extended to study the influence of input variables on the response(s) in any of the machining processes effectively. The modeling technique discussed can be integrated with optimization algorithms.

Acknowledgement

References

[1] Chinmaya, R., Dandekar, D.R., Shin, Y.C. (2011). Molecular dynamics based cohesive zone law for describing Al-SiC interface mechanics, *Composites Part A: Applied Science and Manufacturing*, Vol. 42, No. 4, 355-363, doi: 10.1016/j.compositesa.2010.12.005.

[2] Hung, N.P., Zhong, C.H. (1996). Cumulative tool wear in machining metal matrix composites Part I: Modelling, *Journal of Materials Processing Technology*, Vol. 58, No. 1, 109-113, doi: 10.1016/0924-0136(95)02114-0.

[3] Lin, J.T., Bhattacharyya, D., Kecman, V. (2003). Multiple regression and neural networks analyses in composites machining, *Composites Science and Technology*, Vol. 63, No. 3-4, 539-548, doi: 10.1016/S0266-3538(02)00232-4.

[4] Cramer, D.R., Taggart, D.F. (2002). Design and manufacture of an affordable advanced-composite automotive body structure, In: *Proceedings of 19th International Battery, Hybrid and Fuel Cell Electric Vehicle Symposium & Exhibition*, Busan, Korea, 1-12.

[5] Chandrasekaran, M., Muralidhar, M., Murali Krishna, C., Dixit., U.S. (2010). Application of soft computing techniques in machining performance prediction and optimization: a literature review, *The International Journal of Advanced Manufacturing Technology*, Vol. 46, No. 5-8, 445-464, doi: 10.1007/s00170-009-2104-x.

[6] Hrelja, M., Klancnik, S., Irgolic, T., Paulic, M., Jurkovic, Z., Balic, J., Brezocnik, M. (2014). Particle swarm optimization approach for modelling a turning process, *Advances in Production Engineering & Management*, Vol. 9, No. 1, 21-30, doi: 10.14743/apem2014.1.173.

[7] Abburi, N.R., Dixit, U.S. (2006). A knowledge-based system for the prediction of surface roughness in turning process, *Robotics and Computer-Integrated Manufacturing*, Vol. 22, No. 4, 363-372, doi: 10.1016/j.rcim. 2005. 08.002.

[8] Kohli, A., Dixit, U.S. (2005). A neural-network-based methodology for the surface roughness in a turning process, *The International Journal of Advanced Manufacturing Technology*, Vol. 25, No. 1-2, 118-129, doi: 10.1007/s00170-00 3-1810-z.

[9] Risbood, K.A., Dixit, U.S., Sahasrabudhe, A.D. (2003). Prediction of surface roughness and dimensional deviation by measuring cutting forces and vibrations in turning process, *Journal of Materials Processing Technology*, Vol. 132, No. 1-3, 203-214, doi: 10.1016/s0924-0136(02)00920-2.

[10] Routara, B.C, Sahoo, A.K., Parida, A.K., Padhi, P.C. (2012). Response surface methodology and genetic algorithm used to optimize the cutting condition for surface roughness parameters in CNC turning, *Procedia Engineering*, Vol. 38, 1893-1904, doi: 10.1016/j.proeng.2012.06.232.

[11] Sonar, D.K., Dixit, U.S., Ojha, D.K. (2006). The application of radial basis function for predicting the surface roughness in a turning process, *The International Journal of Advanced Manufacturing Technology*, Vol. 27, No. 7-8, 661-666, doi: 10.1007/s00170-004-2258-5.

[12] Akkuş, H., Asilturk, İ. (2011). Predicting surface roughness of AISI 4140 steel in hard turning process through artificial neural network, fuzzy logic and regression models, *Scientific Research and Essays*, Vol. 6, No. 13, 2729-2736.

[13] Tsao, C.C., Hocheng, H. (2008). Evaluation of thrust force and surface roughness in drilling composite material using Taguchi analysis and neural network, *Journal of Material Processing Technology*, Vol. 203, No. 1-3, 342-348, doi: 10.1016/j.jmatprotec.2006.04.126.

[14] Pradhan, M.K., Biswas, C.K. (2010). Neuro-fuzzy and neural network-based prediction of various responses in electrical discharge machining of AISI D2 steel, *The International Journal of Advanced Manufacturing Technology*, Vol. 50, No. 5-8, 591-610, doi: 10.1007/s00170-010-2531-8.

[15] Muthukrishan, N., Paulo Davim, J. (2009). Optimization of machining parameters of Al-SiC MMC with ANOVA and ANN analysis, *Journal of Materials Processing Technology*, Vol. 209, No. 1, 225-232, doi: 0.1016/j.jmatprotec.2008.01.041.

[16] Basavarajappa, S., Chandramohan, G., Prabu, M., Mukund, K., Ashwin, M. (2007). Drilling of hybrid metal matrix composites—Workpiece surface integrity, *International Journal of Machine Tools Manufacturing*, Vol. 47, No. 1, 92-96, doi: 10.1016/j.ijmachtools.2006.02.008.

[17] Arokiadass, R., Palaniradja, K., Alagumoorthi, N. (2011). Predictive modeling of surface roughness in end milling of Al/SiC$_p$ metal matrix composite, *Archives of Applied Science Research*, Vol. 3, No. 2, 228-236.

[18] Thiagarajan, C., Sivaramakrishan, R., Somasundaram, S. (2011). Cylindrical grinding of SiC particles reinforced aluminium metal matrix composites, *ARPN Journal of Engineering and Applied Sciences*, Vol. 6, No. 1, 14-20.

[19] Korkut, I., Acır, A., Boy, M. (2011). Application of regression and artificial neural network analysis in modeling of tool-chip interface temperature in machining, *Expert Systems with Applications*, Vol. 38, No. 9, 11651-11656, doi: 10.1016/j.eswa.2011.03.044.

[20] Pare, V., Agnihotri, G., A., Krishna, C.M. (2011). Optimization of cutting conditions in end milling process with the approach of particle swarm optimization, *International Journal of Mechanical and Industrial Engineering*, Vol. 1, No. 2, 21-25.

[21] Edwin Raja Dhas, J., Somasundaram, K. (2013). Weld residual stress prediction using artificial neural network and fuzzy logic modeling, *Indian Journal of Engineering & Materials Sciences*, Vol. 18, 351-360.

[22] Devarasiddappa, D., Chandrasekaran, M., Mandal, A. (2012). Artificial neural network modelling for predicting surface roughness in end milling of Al-SiC$_p$ metal matrix composites and its evaluation, *Journal of Applied Sciences*, Vol. 12, No. 10, 955-962, doi: 10.3923/jas.2012.955.962.

[23] Jaya, A.S.M., Hashim, S.Z.M., Rahman, Md.N.A. (2010). Fuzzy logic-based for predicting roughness performance of TiAIN coating, In: *Proceedings of 10th International Conference on Intelligent Systems Design and Applications*, Malaysia, 91-96.

Determining the optimal area-dependent blank holder forces in deep drawing using the response surface method

Volk, M.[a,*]**, Nardin, B.**[a]**, Dolsak, B.**[b]

[a]Gorenje Orodjarna, d.o.o., Velenje, Slovenia
[b]University of Maribor, Faculty of Mechanical Engineering, Maribor, Slovenia

A B S T R A C T

Metal forming processes are often currently highly automated mass production processes for manufacturing a wide variety of metal parts from various industries. Maximizing product quality and consequently minimizing waste and production costs are major goals for those companies exploiting metal forming processes. On the other hand, sheet metal parts become more complex especially because of complex product designs and the usages of higher strength steels that have less formability. Therefore, metal forming processes need to be optimized. This research study demonstrates an optimization system for optimizing the sheet metal forming process using the Finite Element Method (FEM) combined with the Response Surface Method (RSM). The proposed optimization system was tested on an industrial example from the household appliances industry. In this study, it is described as to how to determine optimal area-dependent blank-holder forces in deep drawing process in order to obtain the best possible quality of the drawing part. The optimization system consists of three main steps: modeling, screening, and optimization. The results showed that with better preferences regarding the blank-holder forces, better results can be achieved. Forming and spring-back criteria were taken into account. The number of required numerical simulations using the RSM combined with the Design of Experiment was not critical and was much smaller than using other conventional optimization methods. Therefore, reasonably accurate results can be achieved in a relativity short time, which is one of the main advantages of this method.

1. Introduction

Despite all of the new technologies and improvements in sheet metal forming processes, the forming tools for deep drawing have not significantly changed. The production tools and deep drawing processes are very rigid, therefore it is very hard to improve the quality of the products without extra expenses. On the other hand, deep drawn products become more complex, thus creating additional problems for the toolmakers. Basically, the only (and the most influenced) parameter which can be optimized without encroaching into the tool, and which can be controlled, is a blank holder force (BHF) [1].

Many researchers used BHF for improving the quality of the drawing parts [1-16] and most of them described BHF with the technological window (Fig. 1). An excessive value of BHF causes fracture, whilst an insufficient value of BHF will result in wrinkles [4, 5].
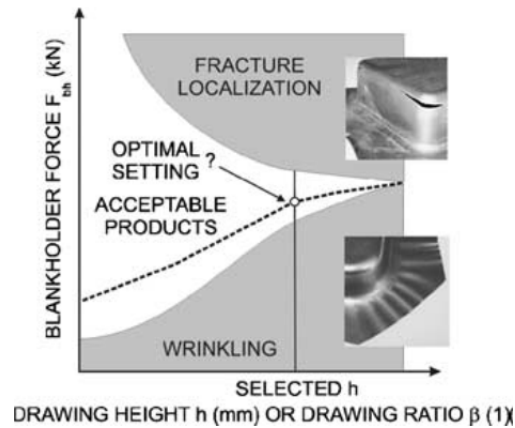
Fig. 1 Technological window [4]

Beside wrinkles and fractures, one of the most important problems is spring-back [10, 12] and the BHF has a large influence on it [9, 13]. Spring-back in sheet-metal forming can be described as the change in the sheet-metal's shape compared with the shapes of the tools after the forming process [8]. We differentiate the following types of spring-back when considering the geometry of a product: angular change, sidewall curl, and twist (Fig. 2).
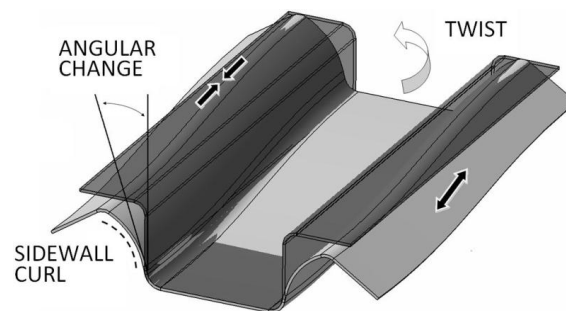
Fig. 2 Types of spring-back [10]

Because BHF seems to be one of the most important parameters in sheet metal forming, a new holding system with segment inserts was developed. This holding system is described in [9, 13] and belongs to holding systems which can provide variable BHFs to the sheet metal [5-8]. While using this holding system, the stamping process is more controlled, the processing window is wider, and the process is more stable [9]. However, finding the optimal configuration of blank holder forces is critical and requires several experimental tests when using conventional optimization methods [5, 9, 15, 16].

This research study presents a method for finding the optimal configuration of blank holder forces. The mathematical approximation algorithm called the response surface method (RSM) and results of finite element numerical simulations were used. Design Expert 8.0 and Pam-stamp 2011 software packages were also used in this research study. The presented method was tested on the deep drawing process but could be used for other applications as well.

2. Used methods

In this research study, the response surface method (RSM) with the combination of finite element method results was used. The response surface methodology is a collection of mathematical and statistical techniques useful for the modeling and analysis of problems in which a response of interest is influenced by several variables, and the objective is to optimize this response [17].
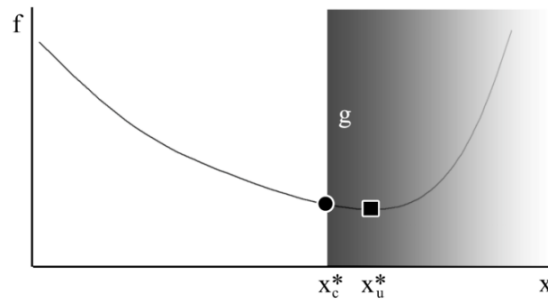
Fig. 3 Mathematical optimization [17]

In general, the optimization method could be described as a mathematical problem in which we are seeking to minimize or to maximize a certain function by systematically choosing the values of certain variables which are allowed to be adopted [18]. Figure 3 presents a function f that needs to be minimized by adopting the variable x. The results of mathematical optimization is the optimum $x_u{}^*$ where function f reaches minimum value. However, in many practical problems, certain restrictions g or unwanted areas (the shaded area in the Fig. 3) are present. If we also take into consideration those restrictions, then the optimum of the mathematical optimization is not at $x_u{}^*$ anymore, but at $x_c{}^*$.

The success of the prediction and optimization critically depends on the ability to develop a suitable approximation for the actual response f of the system. With the RSM the response f is predicted by polynomial models.

A first order polynomial model is given by Eq. 1 [16]

$$y = \beta_0 + \sum_{i=1}^{k} \beta_i x_i + \varepsilon \tag{1}$$

A second order polynomial model also called as quadratic model is given by Eq. 2 [17]

$$y = \beta_0 + \sum_{i=1}^{k} \beta_i x_i + \sum_{i=1}^{k} \beta_{ii} x_i^2 + \sum\sum_{i<j} \beta_{ij} x_i x_j + \epsilon \tag{2}$$

where k is the number of design variables, x_i is the set of design variables, β are polynomial coefficients and $\in$ is minor error.

For many RSM problems, either first or second order models are used. Higher ordered models are not desired due the high amount of experimental data needed for the prediction of the response f.

Nowadays, RSM is used in many applications for solving complex problems which normally requires substantial testing data. In the past, it was also used in some experimental cases of optimizing sheet metal forming processes [19-21].

3. Description of the proposed system

The proposed optimization system consists of 3 main steps: modeling, screening, and optimization (Fig. 4).

The optimization system was developed for deep drawing optimization problems but could also be used for other problems. Some steps can differ or can be skipped in these cases. In the following sections, the optimization system is going to be shown, especially for deep drawing processes.
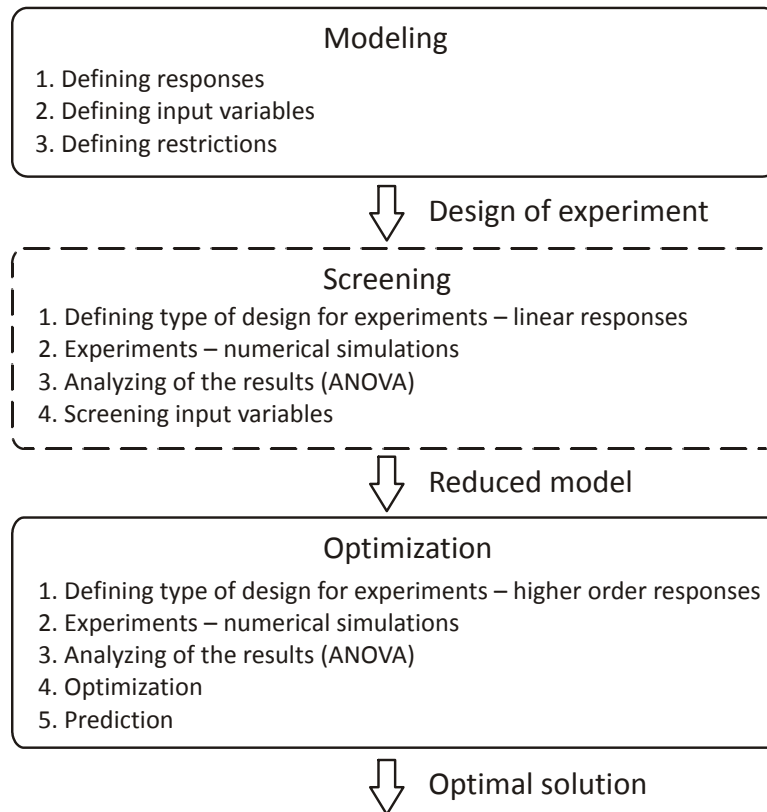
Fig. 4 Proposed optimization system

3.1 Modeling

Modeling is the first step of this optimization procedure. In the modeling step responses, the input variables and restrictions have to be defined. This step depends mostly on the optimization problem which we are going to solve.

Defining responses

In practice, it is common that problems have more than one response. In this research study, we defined responses based on faults which can happen during the deep drawing processes. Many of those faults can be described as forming faults (FF) and faults due to spring-back (FSB), Table 1. Among FF we can include cracks, wrinkles, insufficient stretching and excessive thinning, and into FSB we can count deviations of shape, angular change and twist (Fig. 1 and Fig. 2).

Most of the FF can be well defined based on the forming limit diagram (Fig. 5). The finite element (FE) nodes which lay in area V and VI mean that the product will wrinkle; those which lay in area III will crack and those in IV are safe. Areas I and II are also not desirable because of biaxial tension deformation which can lead to excessive thinning. Therefore, a thinning parameter can be used for avoiding areas I, II, and III.

Table 1 Responses

	Fault	Goal	Fault	Goal	Fault	Goal	Fault	Goal
FF	Wrinkling trend (%)	0 %	Crack (%)	0 %	Insufficient stretching (%)	0 %	Thinning (mm)	Minimum
FSB	Angular change α (°)	0°	Angular change β (°)	0°	Twist (°)	0°	Maximum deviation (mm)	Minimum

Forming Limit Diagram – quality zones
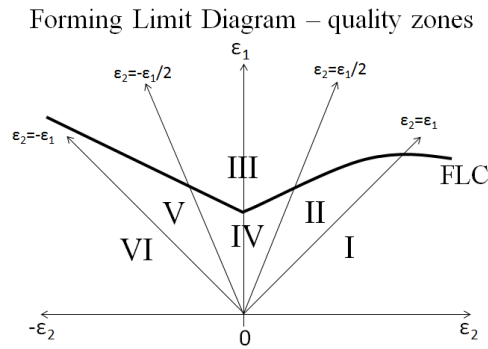
Fig. 5 Forming limit diagram

Among the FSB we can count angular change, twist, and deviations from the reference shape of the drawing part. For this particular part, the angular change was measured in 3 sections (Fig. 6). The sections are equally divided; section 1 is on the symmetry plane, section 2 is 150 mm from the symmetry plane and section 3 is 300 mm from the symmetry plane. The twist was calculated as the angle between plane normal at section 1 and section 3. On the other hand, deviations are represented as the deviation between nodes before and after spring-back. Maximum deviations were taken into consideration.
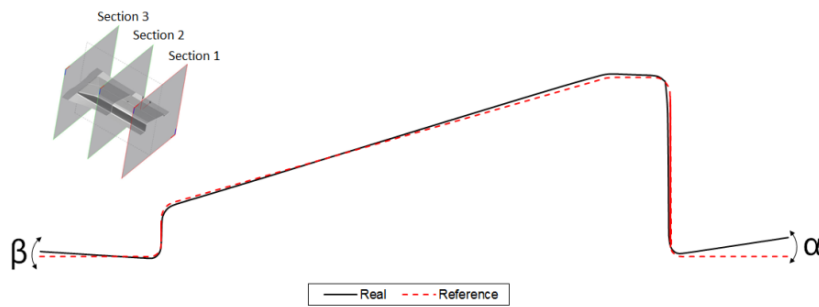
Fig. 6 Spring-back – angular change α and β

Defining input variables

In this research study, the main goal is to optimize the area-dependent BHFs to maximize the part quality of the deep drawing part (Fig. 7). Taking into account the symmetry, the BHF is divided into 6 different areas BHF1, BHF2, BHF3, BHF8, BHF9, and BHF10 which were selected as input variables. In total, this optimization problem therefore consists of 6 different input variables.
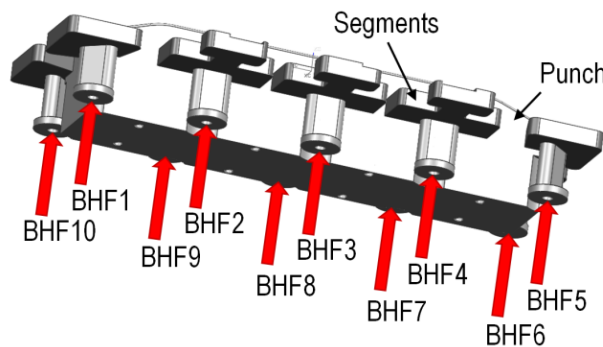
Fig. 7 Input variables – blank holder forces

Defining restrictions

The range of BHFs was determined based on press capability and previous experience. Minimal BHF for each segment was 20 kN and maximal BHF was 60 kN. All ranges and levels of input variables in this study are presented in Table 2.

Table 2 Input variables and their ranges and levels

Factor	Variable	Unit	Min	Mean	Max
A	BHF1	kN	20	40	60
B	BHF2	kN	20	40	60
C	BHF3	kN	20	40	60
D	BHF8	kN	20	40	60
E	BHF9	kN	20	40	60
F	BHF10	kN	20	40	60

3.2 Screening

In this research study, the main goal was to optimize the BHFs. Including the symmetry plane, we had to optimize 6 different BHFs. The main purpose of the screening stage is to minimize the number of input variables. However, there is no need for that in this case because the system is already reduced to only 6 input variables; the number of experimental data is not significantly large and time for numerical simulations is not critical. Therefore, the screening stage was skipped. As this stage was not necessary, it is also marked differently on Fig. 4. This stage seems to be increasingly useful when the complexity of the system grows. The reasonable limit for the RSM is around 8 input variables. If the system consists of more than 8 input variables, then it is advisable to use a screening stage.

The screening stage procedure is very similar to the optimization step with the difference that the screening stage results are analysed on simple linear responses. However, for the optimization higher order polynomials are usually needed. With this simplification, the experimental plans have less data and therefore more input variables can be analysed in a relatively short time, even if the results are not always accurate. However, they are still adequate enough that the trend and the influence of the input variable can be noticed.

3.3 Optimization

Optimization was done based on RSM. Firstly, the experimental plan was made. It was made based on the central composite design (CCD) which gives a good approximation for the second order polynomial. The experimental plan made with CCD consists of $N = 2^k + 2k + N_c$ experiments, where k is the number of input variables and N_C is number of central points. In case in which the results of numerical simulations are used, the central points don't have to be multiplied, therefore the total number of central point is 1. The reason for this is that numerical simulations with the same input parameters will always give the same result. The whole experimental plan can be found in [22] and count to a total of 77 experiments for 6 input variables.

The next step is to analyse the results based on Analysis of Variance (ANOVA) [23]. This step is covered in section 5.1.

The last step of the optimization is to find the optimum input variables in order to increase the quality of the deep drawing part. This can be done using criteria function D (Eq. 3)

$$D = (D_1^{r1} \times D_2^{r2} \times \ldots \times D_n^{ri})^{\frac{1}{\sum ri}}$$ (3)

where D_n is a criterion function for each response, and r_i is the importance of the response. With this optimization method we get a list of solutions, and the solution with the highest number is the best solution. The value of D can be in the range from 0 to 1. Results with $D = 1$ are the solutions which satisfy our goals.

4. Method verification on industry case

The presented method for optimization has been verified on an industry case from the house-hold appliances industry. The main goal in this case was to optimize the quality of the front panel product (Fig. 8). For this purpose, a testing die was made with blank holder with 10 segments inserts (Fig. 7 and Fig. 9). The part is symmetrical in one plane and therefore only half of the part was taken for the investigation.

Fig. 8 Front panel
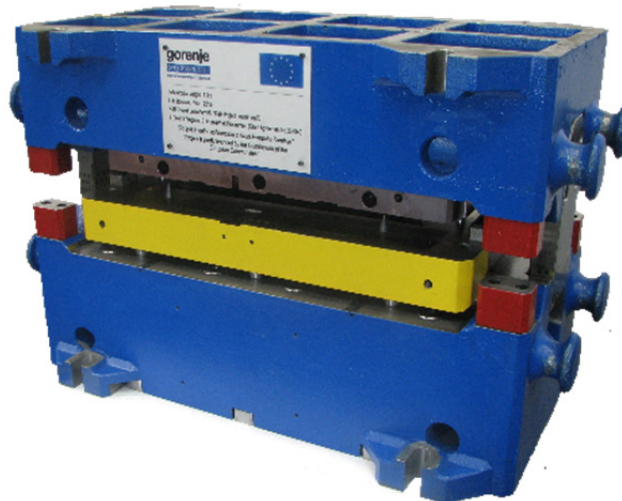
Fig. 9 Testing die

Material properties

A commercially-available DC04 sheet metal with a nominal thickness of 0.7 mm was used for the sheet material.

The material characteristics of the sheet metal have been conducted by uniaxial tensile tests. Tensile tests have been carried out on a Zwick/Roell 1474 machine based on SIST standards. The specimens have been cut at angles 0°, 45°, and 90° with respect to the rolling direction and for each direction five tensile tests have been performed. For the numerical calculations, Hill48 with orthotropic anisotropy was used. The material model's coefficients were identified based on stress-strain curves (Table 3).

Table 3 Material properties of sheet metal

Blank material		DC04
Nominal thickness		0.7 mm
Yield strength		188.9 N/mm^2
Tensile strength		298.4 N/mm^2
Strength coefficient		558.8 N/mm^2
Hardening exponent		0.22
Coefficient of anisotropy	0°	1.67
	45°	1.45
	90°	1.818

The strain-stress hardening curve has been defined by tensile test and extrapolated with Hollomon's hardening law given by Eq. 4 (Fig. 10)

$$\sigma_f = C \times \varepsilon^n \tag{4}$$

where σ_f is yield stress, C is strength coefficient, ε is true strain, and n is hardening exponent.
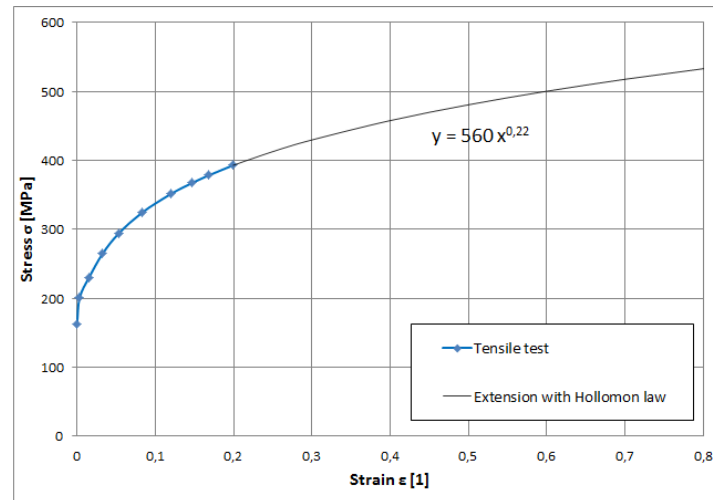
Fig. 10 Strain-stress curve

The forming limit curve (FLC) in Fig. 11 was calculated by the predictive method [24]. The main advantage of this method is that it accurately predicts FLC with the help of mechanical properties A80 which are obtained with the uniaxial tensile test, the *r*-values and the sheet thickness. No other data is needed.
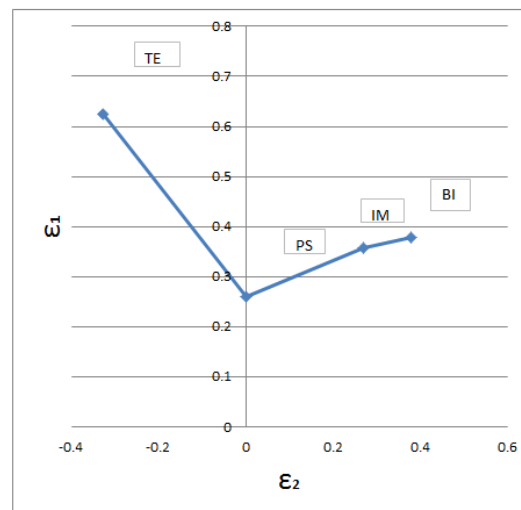
Fig. 11 Forming limit diagram

5. Results and discussion

The results were evaluated to suit the requirements of the selected design of experiments. All the numerical results were analysed through RSM. For this purpose, the quadratic models were mainly used to explain the mathematical relationship between input variables and objective functions. Quadratic polynomial equation for one objective function "thinning" was:

$$Thinning = E^{-5} \times (18459 + 16.8A - 68.5B - 450C - 27.9D + 135.5E + 316.8F - 2.48AD + 2.48AF - 2.96BC + 1.94CD + 2.99CE - 2.9CF + 1.5DE - 3.92DF + 1.9B^2 + 6.26C^2 + 4.04D^2 - 1.89E^2)$$ (5)

5.1 ANOVA

The results of ANOVA presented in this section are presented for only one objective function "thinning". The results for this objective function are shown in Table 4 and indicate that the predictability of the model for thinning is in 99% confidential interval. The predicted responses fit well with those of the numerically obtained results. The coefficients of determination (R^2) values close to 1 indicate that polynomial approximation (Eq. 5) is highly reliable. *F*-value is greater than that of the tabular $F_{0.01}$ [15] and *p*-value is low which suggest that the model influence on the objective function is statistically significant.

Table 4 ANOVA result for the "thinning" objective function in reduced quadratic model

	Sum of squares	Number of factors	Standard deviation	*F*-value	*p*-value
Model	0.032921	18	0.001829	21.6705	< 0.0001
A-BHF1	8.37E-06	1	8.37E-06	0.099115	0.7540
B-BHF2	0.000754	1	0.000754	8.939431	0.0041
C-BHF3	0.006624	1	0.006624	78.48896	< 0.0001
D-BHF8	0.008627	1	0.008627	102.221	< 0.0001
E-BHF9	0.000914	1	0.000914	10.83443	0.0017
F-BHF10	0.005354	1	0.005354	63.44184	< 0.0001
AD	0.000327	1	0.000327	3.875955	0.0538
AF	0.000159	1	0.000159	1.879241	0.1757
BC	0.000964	1	0.000964	11.4271	0.0013
CD	0.00034	1	0.00034	4.029295	0.0494
CE	0.000917	1	0.000917	10.86932	0.0017
CF	0.000436	1	0.000436	5.171731	0.0267
DE	0.000229	1	0.000229	2.709674	0.1052
DF	0.000785	1	0.000785	9.305206	0.0034
B^2	0.000254	1	0.000254	3.004378	0.0884
C^2	0.002791	1	0.002791	33.07372	< 0.0001
D^2	0.001108	1	0.001108	13.12282	0.0006
E^2	0.000225	1	0.000225	2.66841	0.1078

R^2=0.870555665; Adj. R^2=0.830383285; pred. R^2=0.776865668

5.2 Optimization

Optimization is made based on the results which are predicted by the polynomial. The optimization system predicts a set of solutions with different BHFs and belonging values of objective functions. All results can be presented graphically with the response surface (Fig. 12). This Figure presents results based on BHF4, BH6 and desirability which is a parameter describing the achievement of our goals. It is calculated by Eq. 2. The solution on the top of the surface presents the best solution with a highest value of D. All input parameters for these solutions are shown in Table 5.

Table 5 Best solution chosen based on desirability

Variable	BHF1	BHF2	BHF3	BHF8	BHF9	BHF10
Value (kN)	43	54	35	48	60	30
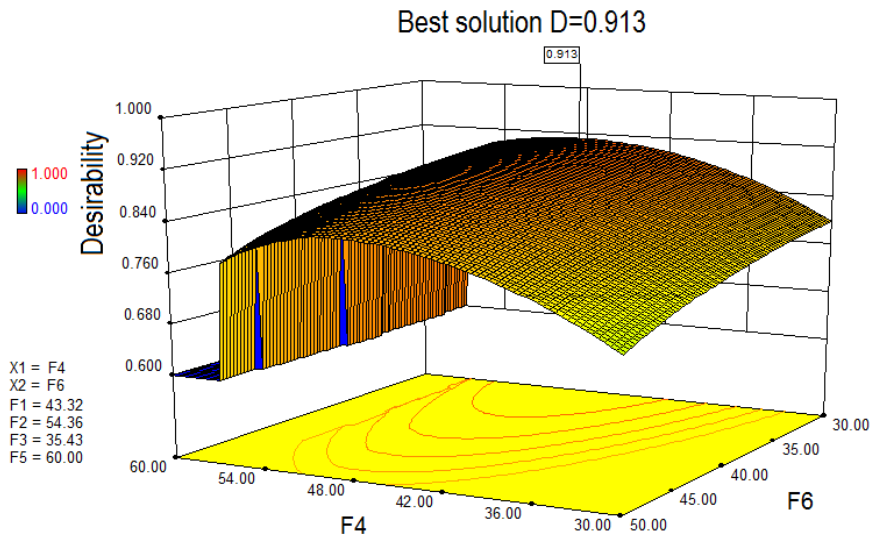
Fig. 12 Response surface of all solutions

5.3 Comparing with FEM results

At the end of this research study, we checked if the optimal solution is really better than the previous one. We checked this by comparing numerical results made with BHFs before and after this optimization. This comparison is described in Fig. 13 and in Table 6. The results showed a significant improvement of all quality parameters. This has proven the usefulness of the presented method, and its great potential for the optimization of sheet metal forming processes.
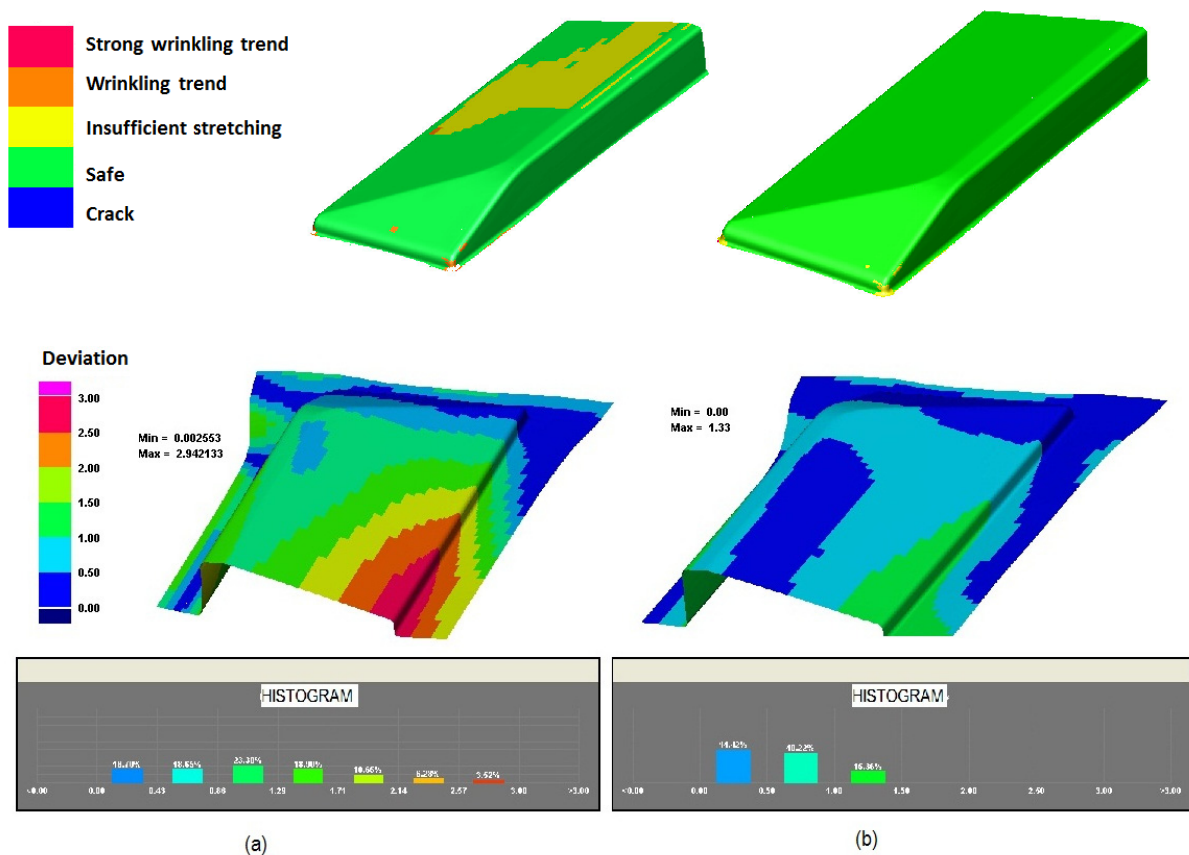
Fig. 13 Comparison of the results before and after optimisation

Table 6 Comparing numerical results before and after optimisation

Objective function	Wrinkling trend	Crack	Insufficient stretching	Thinning	Maximum deviation
Before optimization	2.27 %	0.02 %	24.08 %	21.5 %	2.94
After optimization	0.42 %	0 %	0 %	20.9 %	1.33
Improvements	+82 %	-	+100 %	+3 %	+55 %

Fig 13. graphically shows improvement in the part quality. The upper two figures show that more area which represents safe area (FE nodes which lay in area IV on Fig 5.) is present on the right part. The lower two figures show deviations between FE nodes before and after springback. The right optimized part has fewer deviations.

Even better improvements can be seen in Table 6. The improvements shown are significant. For the quality parameter "crack" the improvements in % is not calculated because the defect after optimization is 0 % and even before optimization the % was very low.

Reported results show that by using this optimization system, reasonably good results and improvements can be achieved in a relatively short time. This optimization can be done during the development of the manufacturing method for the part, which could be a substantial benefit later in the production. The accuracy of the results strongly depends on the accuracy of the numerical models. However, numerical simulations are becoming increasingly reliable; therefore, this optimization system will become even more valuable.

6. Conclusion

This research study presents the newly developed optimization system for optimising deep drawing parameters in order to get better part quality. The optimization system consists of three steps: modeling, screening and optimization. The methodology incorporates RSM and the results of FEM; the optimum area-dependent BHFs are determined with FEM and RSM by optimizing the objective function related with variables that are very difficult to determine during try-outs, as well as very time consuming.

At the end of this research study, the optimization system was tested on the industrial example from the household appliances industry. It took into account the most important input variables and unwanted output properties (as objective functions) of the part. Results showed that with optimization of the process and area-dependent BHF, that it is possible to achieve the better part quality. The optimization system was developed for deep drawing optimization problems, but could also be used for other problems in various fields.

Acknowledgement

References

[1] Tisza, M. (2013). Recent development trends in sheet metal forming, *International Journal of Microstructure and Materials Properties,* Vol. 8, No. 1/2, doi: 10.1504/IJMMP.2013.052651.
[2] Albut, A., Ciubotaru, V., Radu, C., Olaru, I. (2011). Optimization of the blank holder force using neural network algorithm, In: *AIP Conf. Proc. 1383*, Vol. 1383, 1004-1009, doi: 10.1063/1.3623714.
[3] Liewald, M., Wurster, K., Blaich, C. (2011). New approaches on automated wrinkle detection in sheet metal components by forming simulation, In: *AIP Conf. Proc. 1353,* 1185-1190, doi: 10.1063/1.3589677.
[4] Gantar, G., Kuzman, K., Filipič, B. (2005). Increasing the stability of the deep drawing process by simulation-based optimization, *Journal of Materials Processing Technology,* Vol. 164-165, 1343-1350, doi: 10.1016/j.jmatprotec.2005.02.099.
[5] Kitayama, S., Hamano, S., Yamazaki, K., Kubo, T., Nishikawa, H., Kinoshita, H. (2010). A closed-loop type algorithm for determination of variable blank holder force trajectory and its application to square cup deep drawing, *The International Journal of Advanced Manufacturing Technology,* Vol. 51, No. 5-8, 507-517, doi: 10.1007/s00170-010-2656-9.

[6] Palaniswamy, H., Braedel, M., Thandapani, A., Altan, T. (2006). Optimal programming of multi-point cushion systems for sheet metal forming, *CIRP Annals – Manufacturing Technology,* Vol. 55, No. 1, 249–254, doi: 10.1016/S0007-8506(07)60409-0.

[7] Neugebauer, R., Leib, U., Bräunlich, H., (1997). Influence on materials flow in deep drawing using individual controllable draw pins and smooth blankholder design, In: *Proceedings of SAE International Congress & Exposition*, Detroit, Michigan, SEA Paper No. 970989, 269-274, doi: 10.4271/970989.

[8] Endelt, B., Tommerup, S., Danckert, J. (2009). A novel feedback control system – Controlling the material flow in deep drawing using distributed blank-holder force, *Journal of Materials Processing Technology,* Vol. 213, No. 1, 36–50, doi: 10.1016/j.jmatprotec.2012.08.003.

[9] Volk, M., Deželak, M., Nardin, B., Stepišnik, S. (2012). Prediction of the spring-back calculated with numerical simulations for the household industry, In: *AIP Conf. Proc. 1383*, 1078-1085, doi: 10.1063/1.3623723.

[10] Deželak, M., Pahole, I., Stepišnik, A., Fijavž, R. (2011). Finite element method combined with machine learning for springback prediction, In: *6th International Conference and Exhibition on Design and Production of Machines and Dies/Molds,* Atilim University, Ankara, Turkey, 83-87.

[11] Dezelak, M., Stepisnik, A., Pahole, I., Ficko, M. (2014). Evaluation of twist springback prediction after an AHSS forming process, *International Journal of Simulation Modelling*, Vol. 13, No. 2, 171-182, doi: 10.2507/IJSIMM13(2)4.261.

[12] Tang, L., Wang, H., Li, G. (2013). Advanced high strength steel springback optimization by projection-based heuristic global search algorithm, *Materials & Design,* Vol. 43, 426-437, doi: 10.1016/j.matdes.2012.06.045.

[13] Volk, M., Nardin, B., Dolšak, B. (2011). Application of numerical simulations in the deep-drawing process and the holding system with segments' inserts, *Strojniški vestnik – Journal of Mechanical Engineering,* Vol. 57, 697-703, doi: 10.5545/sv-jme.2010.258.

[14] Albut, A., Ciubotaru, V., Radu, C., Olaru, I. (2011). Optimization of the blank holder force using the neural network algorithm, In: *AIP Conf. Proc.* 1383, 1004-1009, doi: 10.1063/1.3623714.

[15] Intarakumthornchai, T., Jirathearanat, S., Juntaratin, J. (2011). Determination of loading paths in hydromechanical deep drawing process of parabolic cup with FEA based 2-D interval halving and fuzzy logic, In: *Proceedings of the 4th International Conference on Modelling and Simulation of Metallurgical Processes in Steelmaking – Metec Insteelcon 2011,* Düseldorf, Germany.

[16] Kitayama, S., Kita, K., Yamazaki, K. (2012). Optimization of variable blank holder force trajectory by sequential approximate optimization with RBF network, *The International Journal of Advanced Manufacturing Technology,* Vol. 61, No. 9-12, 1067-1083, doi: 10.1007/s00170-011-3755-y.

[17] Montgomery, D.C. (2012). *Design and analysis of experiments*, 5th ed*., Wiley,* New York.

[18] Bonte, M.H.A. (2007). Optimisation strategies for metal forming processes, PhD Thesis, University of Twente, Enschede, The Netherlands.

[19] Intarakumthornchai, T., Jirathearanat, S., Thongprasert, S., Dechaumphai, P. (2010). FEA based optimization of blank holder force and pressure for hydromechanical deep drawing of parabolic cup using 2-D interval halving and RSM methods, *Engineering Journal,* Vol. 14, No. 2, 15-32, doi: 10.4186/ej.2010.14.2.15.

[20] Velmanirajan, K., Thaheer, A.S.A., Narayanasamy, R., Ahamed Basha, C. (2012). Numerical modelling of aluminium sheets formability using response surface methodology, *Materials & Design,* Vol. 41, 239-254, doi: 10.1016/j.matdes.2012.05.027.

[21] Sun, G., Li, G., Gong, Z., Cui, X., Yang, X., Li, Q. (2010). Multiobjective robust optimization method for drawbead design in sheet metal forming, *Materials & Design,* Vol. 31, No. 4, 1917-1929, doi: 10.1016/j.matdes.2009.10.050.

[22] Volk, M. (2013). Stabilization of the deep drawing process with sheet metal holding control, PhD Thesis, (original title: Stabilizacija procesa globokega vleka z obvladovanjem pridrževanja pločevine), University of Maribor, Faculty of mechanical engineering, Maribor, Slovenia.

[23] Hribernik, A. (2011). Methods of experimental work: design of experiments (original title: Metode eksperimentalnega dela: načrtovanje eksperimentov), University of Maribor, Faculty of mechanical engineering, Maribor, Slovenia.

[24] Abspoel, M., Scholting, M.E., Droog, J.M.M. (2012). A new method for predicting forming limit curves from mechanical properties, *Journal of Materials Processing Technology*, Vol. 213, No. 5, 759-769, doi: 10.1016/j.jmatprotec.2012.11.022.

Imprecise data envelopment analysis model for robust design with multiple fuzzy quality responses

Al-Refaie, A.[a,*], **Li, M.-H.**[b], **Jarbo, M.**[a], **Yeh, C.-H.B.**[b], **Nour, B.**[a]

[a]Department of Industrial Engineering, The University of Jordan, Amman, Jordan
[b]Department of Industrial Engineering and Systems Management, Feng Chia University, Taichung, Taiwan

A B S T R A C T

In this research, Imprecise Data Envelopment Analysis (IDEA) model was utilized to improve fuzzy multiple responses in robust design. The combination of process factor levels at each experiment was considered as a Decision Making Unit (DMU) with responses treated as inputs and outputs for all DMUs. The Fuzzy C-Means Clustering (FCMC) technique is used to fit the response fuzziness by clustering the average values, relative to each response, into a suitable number of clusters with triangular / trapezoidal membership functions. IDEA models were used to estimate the fuzzy triangular / trapezoidal efficiency values for each DMU. Finally, the preference degree-based ranking approach was used to discriminate between the fuzzy efficiency values and identifying the best combination of factors levels that would improve fuzzy multiple responses. Two case studies are utilized to illustrate the proposed approach, including optimizing wire electrical discharge machining and sputtering process parameters. The results showed that the proposed approach provides better anticipated improvements than the fuzzy multiple regression based approach. This approach would provide great assistant to process engineers in improving process performance with fuzzy multiple responses over a wide range of business applications.

1. Introduction

To survive in today's competitive markets, manufacturers produce their products considering multiple quality responses of main customer interest. Therefore, engineers aim to determine the best combination of process settings that reduces the variability of the quality responses and simultaneously shift the mean to the desired target [1]. For this reason, several approaches are proposed to optimize product/process performance with multiple responses [2-8].

In reality, dealing with response fuzziness becomes a challenging task for process engineers. The fuzzy responses are captured as an imprecise value rather than crisp one. The imprecise value could be interval, triangular, trapezoidal, or even linguistic. Conceptually, response fuzziness can be justified by four reasons [9, 10]. The first reason is the vague and complex process behaviour which may be explained by the nondiscretionary factors. The second is the inability to fix the process settings at precise values or in words the fuzziness inherent in the settings physical values. The third is the qualitative nature of the response itself. Finally, the fuzziness occurs due to customer preference. Several approaches are proposed to deal with response fuzziness problem in robust design [9-16].

The Taguchi method utilizes an orthogonal array to provide experimental format. Let DMU_j denotes the combination of factor settings at each experiment in Taguchi's orthogonal array. For DMU_j, the fuzzy inputs and outputs are denoted by $\breve{y}_{ij}$ and $\breve{y}_{rj}$, respectively. In fuzzy goal programming (FGP), the fuzzy efficiency value, $\breve{E}_j$, of each DMU_j is calculated as follows. For a fuzzy triangular inputs, $\breve{y}_{ij}$, and outputs, $\breve{y}_{rj}$, values, the relative efficiency value of each DMU_j is also considered as a fuzzy triangular value with three parameters, E_j^L, E_j^M, and E_j^U, which represent the lower, nominal, and the upper efficiency values, respectively. That is, $\widetilde{E}_j = (E_j^L, E_j^M, E_j^U)$ and is formulated as shown in Eq. 1:

$$\tilde{E}_j = \begin{cases} \dfrac{\sum_{r=1}^{s} u_r\, y_{rj}^L}{\sum_{i=1}^{m} vi\, y_{ij}^U} \\[2em] \dfrac{\sum_{r=1}^{s} u_r\, y_{rj}^M}{\sum_{i=1}^{m} v_i\, y_{ij}^M} \\[2em] \dfrac{\sum_{r=1}^{s} u_r\, y_{rj}^U}{\sum_{i=1}^{m} v_i\, y_{rj}^L} \end{cases} \tag{1}$$

where s and m denote the number of outputs and inputs, respectively. Let the lower and upper inputs values are denoted by y_{ij}^L and y_{ij}^U, respectively. Also, the lower and upper outputs values are expressed as y_{rj}^L and y_{rj}^U, respectively. For a DMU, $DMU_{k \in j}$, under consideration, the upper desired efficiency value, E_k^U, is calculated by using Model 1.

Model 1 is:

$$E_k^U = max \sum_{r=1}^{s} u_r\, y_{rk}^U \tag{2}$$

subject to

$$\sum_{i=1}^{m} v_i\, y_{ik}^L = 1 \tag{3}$$

$$\sum_{r=1}^{s} u_r y_{rk}^U - \sum_{i=1}^{m} v_i\, y_{ik}^L \leq 0 \tag{4}$$

$$\sum_{r=1}^{s} u_r y_{rj}^L - \sum_{i=1}^{m} v_i\, y_{ij}^U \leq 0, \quad \forall\, j \neq k \tag{5}$$

$$u_r, v_i \geq \varepsilon, \forall\, r, i \in q \tag{6}$$

where u_r, and v_i, are the weights assigned to the outputs and inputs, and ε is the non-Archimedean value. In model 1, the objective function seeks to maximize the upper relative efficiency for each DMU_k under the most favorable situation. The first constraint keeps the inputs weighted sum of the DMU_k equals one. The second and the third constraints represent the most favorable condition for DMU_k, where the highest score of the upper efficiency value is attained by settings the relative interval outputs at their upper bounds and the interval inputs at their lower bounds. Meanwhile, the outputs of all other $DMU_{j \neq k}$ reach their corresponding lower bounds and the interval inputs reach their corresponding upper bounds. The last constraint keeps the inputs and outputs weights larger than a small positive value. Similarly, the lower efficiency value E_k^L, is calculated by using Model 2.

Model 2 is:

$$E_k^L = max \sum_{r=1}^{s} u_r \, y_{rk}^L \tag{7}$$

subject to

$$\sum_{i=1}^{m} v_i \, y_{ik}^U = 1 \tag{8}$$

$$\sum_{r=1}^{s} u_r y_{rk}^L - \sum_{i=1}^{m} v_i \, y_{ik}^U \leq 0 \tag{9}$$

$$\sum_{r=1}^{s} u_r y_{rj}^U - \sum_{i=1}^{m} v_i \, y_{ij}^L \leq 0, \quad \forall \, j \neq k \tag{10}$$

$$u_r, v_i \geq \varepsilon \,, \forall \, r, i \tag{11}$$

In Model 2, the objective function seeks to maximize the lower relative efficiency E_k^L, for each DMU_k under the least favorable situation. The first constraint keeps the upper weighted sum of the DMU_k inputs equals one. The second and the third constraints represent the least favorable condition for DMU_k, where the highest score of the relative efficiency value is attained by setting the relative interval outputs at their lower bounds and the interval inputs at the upper bounds, while the interval outputs of all other $DMU_{j\neq k}$ reach their relative upper bounds and the interval inputs reach their corresponding lower bounds. The last constraint keeps the inputs and outputs weights larger than a small positive value.

Further, let the middle inputs and outputs values are denoted by y_{ij}^M and y_{rj}^M, respectively. Then, for DMU_k the nominal efficiency value, E_k^M, is calculated by using Model 3 as follows:

Model 3 is:

$$E_k^M = max \sum_{r=1}^{s} u_r \, y_{rk}^M \tag{12}$$

subject to

$$\sum_{i=1}^{m} v_i \, y_{ik}^M = 1 \tag{13}$$

$$\sum_{r=1}^{s} u_r y_{rk}^M - \sum_{i=1}^{m} v_i \, y_{ik}^M \leq 0, \quad j = k \tag{14}$$

$$\sum_{r=1}^{s} u_r y_{rj}^U - \sum_{i=1}^{m} v_i \, y_{ij}^L \leq 0, \quad \forall \, j \neq k \tag{15}$$

$$u_r, v_i \geq \varepsilon \,, \forall \, r, i \in q \tag{16}$$

The objective function in Model 3 seeks the optimal setting of outputs and inputs weights, u_r and v_i, that maximize the nominal efficiency value, E_k^M, for each DMU_k. The second and the third constraints keep the input weighted sum for each DMU_k constant and at the same time the relative efficiency value less than one. The fourth constraint represents the nominal desired condition for each DMU_k such that the nominal efficiency value is achieved when its relative outputs and inputs values reach their middle level, while the outputs reach their corresponding higher levels and the inputs reach their corresponding lower levels for $DMU_{j\neq k}$. The last constraint keeps the values of the inputs and outputs weights more than a small non Archimedean variable.

On the other hand, for a fuzzy trapezoidal inputs, $\breve{y}_{ij}$ and outputs $\breve{y}_{rj}$, values the relative efficiency value of each DMU_j have four parameters, E_j^L, E_j^{LM}, E_j^{UM}, and E_j^U which represent the lower, lower mid, upper mid, and the upper efficiency values, respectively. The fuzzy trapezoidal efficiency value of each DMU_j can be written as $\tilde{E}_j = (E_j^L, E_j^{LM}, E_j^{UM}, E_j^U)$ which is shown in Eq. 17.

$$\tilde{E}_j = \begin{cases} \dfrac{\sum_{r=1}^{s} u_r \, y_{rj}^L}{\sum_{i=1}^{m} v_i \, y_{ij}^U} \\[2em] \dfrac{\sum_{r=1}^{s} u_r \, y_{rj}^{LM}}{\sum_{i=1}^{m} v_i \, y_{ij}^{LM}} \\[2em] \dfrac{\sum_{r=1}^{s} u_r \, y_{rj}^{UM}}{\sum_{i=1}^{m} v_i \, y_{ij}^{UM}} \\[2em] \dfrac{\sum_{r=1}^{s} u_r \, y_{rj}^{U}}{\sum_{i=1}^{m} v_r \, y_{rj}^{L}} \end{cases} \tag{17}$$

Then, Model 1 and Model 2 are used to calculate the upper and lower relative efficiencies for each DMU_j, respectively. The lower mid efficiency value, E_j^{LM}, is calculated as follows:

Model 4 is:

$$E_k^{LM} = max \sum_{r=1}^{s} u_r \, y_{rk}^{LM} \tag{18}$$

subject to

$$\sum_{i=1}^{m} v_i \, y_{ik}^{LM} = 1 \tag{19}$$

$$\sum_{r=1}^{s} u_r y_{rk}^{LM} - \sum_{i=1}^{m} v_i \, y_{ik}^{LM} \leq 0, \tag{20}$$

$$\sum_{r=1}^{s} u_r y_{rj}^{U} - \sum_{i=1}^{m} v_i \, y_{ij}^{L} \leq 0, \quad j \neq k \tag{21}$$

$$u_r, v_i \geq \varepsilon, \forall \, r, i \in q \tag{22}$$

In Model 4, the lower mid values of the inputs are set as $\bar{y}_{ij}^{LM}$, while the lower mid values of the outputs are set as $\bar{y}_{rj}^{LM}$. The objective function seeks the optimal setting of outputs and inputs

weights u_r, v_i that maximize the relative efficiency value, E_k^{LM}, for each DMU_k. The second and the third constraints keep the lower mid efficiency value for each DMU_k less than one and the input weighted sum equal to one. The fourth constraint represents the lower mid desired condition for each DMU_k such that the lower mid efficiency value is achieved when its relative outputs and inputs values are at their lower mid-level, while the outputs and inputs for $DMU_{j\neq k}$ are at their corresponding higher and lower relative levels respectively. The last constraint keeps the values of the inputs and outputs weights larger than a small non Archimedean variable [17].

By the same way, the upper mid efficiency value, E_k^{UM}, is calculated by using Model 5 as follows.

Model 5 is:

$$E_k^{UM} = max \sum_{r=1}^{s} u_r y_{rk}^{UM} \tag{23}$$

subject to

$$\sum_{i=1}^{m} v_i y_{ik}^{UM} = 1 \tag{24}$$

$$\sum_{r=1}^{s} u_r y_{rk}^{UM} - \sum_{i=1}^{m} v_i y_{ik}^{UM} \leq 0, \tag{25}$$

$$\sum_{r=1}^{s} u_r y_{rj}^{U} - \sum_{i=1}^{m} v_i y_{ij}^{L} \leq 0, \quad j \neq k \tag{26}$$

$$u_r, v_i \geq \varepsilon, \forall\, r, i \in q \tag{27}$$

Utilizing the Models 1 to 5, the optimal factor settings can then be determined. Therefore, this research proposes an extension to ongoing research by proposing a procedure for solving the fuzzy multiple responses problem in robust design using DEA approaches. The remaining of this research including introduction is organized as follows. Section two presents the proposed approach. Section three illustrates the proposed approach using two cases. Section four compares the results. Finally, section four highlights the research conclusions.

2. The proposed approach

In robust design method, several combinations of process factor levels are conducted to determine the best combination that improves multiple responses of main concern. The proposed approach for solving the multiple fuzzy quality characteristics is outlined in the following steps:

Step 1: Let y_{qj} denotes the value of the q-th response at the j experiment. Then, the combination of factor levels at each experiment is treated as a DMU_j. Let $\bar{y}_{qj}$ be the response average of the-smaller-the-better (STB), the-larger-the-better (LTB) response or the quality loss value for the-nominal-the-best (NTB) response to a number of triangular or trapezoidal membership functions.

Step 2: The FCMC technique is used to cluster the average values of $\bar{y}_{qj}$ into a number of classes, d, each is treated either as a triangular or trapezoidal membership function. The parameter of each membership function is determined such that, the class center, c_{qd}, for the triangular membership function is considered as the most likely value, $\bar{y}_{qd}^{M}$. The upper, $\bar{y}_{qd}^{U}$, and lower, $\bar{y}_{qd}^{L}$, pa-

rameters are determined by the centers of the neighbor classes or the DMU with least considerable membership value. For the trapezoidal membership function, the lower mid, $\bar{y}_{qd}^{LM}$, and the upper mid, $\bar{y}_{qd}^{UM}$, of each class are considered as the DMUs of the largest membership value relative to the same class. The upper and lower parameters $\bar{y}_{qd}^{U}$ and $\bar{y}_{qd}^{L}$, are determined by the centers of the neighbor classes or the DMU with least considerable membership value.

Step 3: The fuzzy efficiency values are computed by using models 1 to 5. The upper mid values inputs are set as y_{ij}^{UM} and the upper mid outputs are set y_{rj}^{UM} in Model 5, which has similar to that of Model 4 except the fourth constraint represents the upper mid desired condition for each DMU_k where the upper mid efficiency value is achieved when its relative outputs and inputs values are at their upper mid-level, while the outputs and inputs reach their corresponding higher and lower levels respectively for $DMU_{j \neq k}$.

Step 4: The preference degree based ranking approach [18] is used for clear-cut discrimination among the DMUs. In this regard, the complete ranking order for *n* fuzzy efficiency values can be obtained as (1) the triangular efficiency values and (2) the trapezoidal efficiency values.

(1) For the triangular efficiency values:

In the preference degree based ranking approach, let $\tilde{E}_k = (E_k^L, E_k^M, E_k^U)$ and $\tilde{E}_{j \neq k} = (E_j^L, E_j^M, E_j^U)$, are two fuzzy triangular efficiency values. According to fuzzy arithmetic, there are four possible relationships to compare $\tilde{E}_k$ with $\tilde{E}_{j \neq k}$ as shown in Eq. 28.

$$P\big(\tilde{E}_k > \tilde{E}_{j \neq k}\big) =$$

$$= \begin{cases} 1, & \text{IF } (E_k^L \geq E_{j \neq k}^U) \\ 0, & \text{IF } (E_k^U \leq E_{j \neq k}^L), \\ \dfrac{\big(E_k^U - E_{j \neq k}^L\big)^2}{\big(E_k^U - E_{j \neq k}^L + E_{j \neq k}^M - E_k^M\big)\big(E_k^U - E_k^L + E_{j \neq k}^U - E_{j \neq k}^L\big)}, & \text{IF } (E_k^U > E_{j \neq k}^L) \cap (E_k^M \leq E_{j \neq k}^M), \\ \dfrac{\big(E_{j \neq k}^U - E_k^L\big)^2}{\big(E_{j \neq k}^U - E_k^L + E_k^M - E_{j \neq k}^M\big)\big(E_k^U - E_k^L + E_{j \neq k}^U - E_{j \neq k}^L\big)}, & \text{IF } (E_k^L < E_{j \neq k}^U) \cap (E_k^M > E_{j \neq k}^M). \end{cases} \quad (28)$$

The preference matrix $P_{k,j}$ is calculated as follows:

$$\boldsymbol{P_{k,j}} = \begin{bmatrix} p_{k,j} & \breve{E}_{j=1} & \tilde{E}_{j=k} & \tilde{E}_{j=n} \\ \tilde{E}_{j=1} & 0.5 & p_{1,k} & p_{1,n} \\ \tilde{E}_{j=k} & \dots & 0.5 & p_{k,n} \\ \tilde{E}_{J=n} & \dots & \dots & 0.5 \end{bmatrix} \quad (29)$$

where $\boldsymbol{P_{k,j}}$ is the preference matrix for all DMUs. Find a row from the matrix, $\boldsymbol{P_{k,j}}$, whose elements except the diagonal are larger than or equal to 0.5. If this row corresponds to $\tilde{E}_k$, then DMU_k is considered as the most efficient DMU and its relative settings are the best. The kth row is eliminated from the matrix. In the reduced matrix, if $\tilde{E}_{h \neq k}$ stands out with the largest preference values compared to the remaining efficiency values, then $\tilde{E}_{h \neq k}$ is ranked in the second place. Repeat this step until all of the fuzzy efficiency values are properly ranked.

(2) For the trapezoidal efficiency values:

Let $\tilde{E}_k(E_k^L, E_k^{LM}, E_k^{UM}, E_k^U)$ and $\tilde{E}_{j \neq k}(E_{j \neq k}^l, E_{j \neq k}^{LM}, E_{j \neq k}^{UM}, E_{j \neq k}^U)$ be two fuzzy trapezoidal efficiency values. According to fuzzy arithmetic, there are five possible relationships to compare $\tilde{E}_k$ with $\tilde{E}_{j \neq k}$, which are stated in Eq. (30).

$$P\big(\tilde{E}_k > \tilde{E}_{j\neq k}\big) =$$

$$= \begin{cases} 1, & IF\ (E_k^L \geq E_{j\neq k}^U) \\ 0, & IF\ (E_k^U \leq E_{j\neq k}^L) \\ \dfrac{(E_k^u - E_{j\neq k}^l)^2}{(E_k^U - E_{j\neq k}^L + E_{j\neq k}^{ML} - E_k^{MU})(E_k^U - E_k^L + E_k^{MU} - E_k^{ML} + E_{j\neq k}^{MU} - E_{j\neq k}^{ML} + E_{j\neq k}^U - E_{j\neq k}^L)}, & (E_k^U > E_{j\neq k}^{LM}) \cap (E_k^{UM} \leq E_{j\neq k}^{LM}) \\ \dfrac{(E_k^u - E_{j\neq k}^l + E_k^{UM} - E_{j\neq k}^{LM})}{(E_k^U - E_k^L + E_k^{MU} - E_k^{ML} + E_{j\neq k}^{MU} - E_{j\neq k}^{ML} + E_{j\neq k}^U - E_{j\neq k}^L)}, & (E_k^{UM} > E_{j\neq k}^{LM}) \cap (E_k^{LM} \leq E_{j\neq k}^{UM}) \\ \dfrac{(E_{j\neq k}^u - E_j^l)^2}{(E_{j\neq k}^u - E_k^l + E_k^{ml} - E_{j\neq k}^{mu})(E_k^U - E_k^L + E_k^{MU} - E_k^{ML} + E_{j\neq k}^{MU} - E_{j\neq k}^{ML} + E_{j\neq k}^U - E_{j\neq k}^L)}, & (E_k^{LM} > E_{j\neq k}^{UM}) \cap (E_k^L < E_{j\neq k}^U) \end{cases} \quad (30)$$

The preference matrix, $\boldsymbol{P_{k,j}}$, is calculated using Eq. (30):

$$\boldsymbol{P_{k,j}} = \begin{bmatrix} p_{k,j} & \breve{E}_{j=1} & \tilde{E}_{j=k} & \tilde{E}_{j=n} \\ \tilde{E}_{j=1} & 0.5 & p_{1,k} & p_{1,n} \\ \tilde{E}_{j=k} & \dots & 0.5 & p_{k,n} \\ \tilde{E}_{J=n} & \dots & \dots & 0.5 \end{bmatrix} \quad (31)$$

where $\boldsymbol{P_{k,j}}$ is the preference matrix for all DMUs. Repeat until all of the fuzzy efficiency values are properly ranked.

Step 5: The anticipated improvements are calculated by using the proposed approach, then the improvements gained by the proposed approach are compared to fuzzy multiple regression approach (FMRA).

3. Two cases for illustration

Two cases adopted in the literature are applied to illustrate the proposed approach. The first case deals with response fuzziness that is best fit by fuzzy triangular membership function, whereas the second case considers trapezoidal membership function as the best fit to response fuzziness.

3.1 Case I: Optimization of Inconel on machining of CNC WEDM process

Al-Refaie et al. [8] conducted nine experiments utilizing Taguchi's L9 array to optimize the multi quality responses of Inconel 718 on machining of CNC WEDM process using fuzzy multiple regression approach (FMRA). The two quality responses are surface roughness (SR), y_1, which is a STB type response and material removal rate (MRR), y_2, which is a LTB type response. Table 1 shows the four process factors considered which are: pulse in time (A), delay time (B), wire feed speed (C), ignition current (D) as well as the corresponding levels. The combination of factor settings at each experiment is treated as DMU_j, where the average values of SR, $\bar{y}_{1j}$, are considered as inputs, while the average values of MRR, $\bar{y}_{2j}$, are the outputs for DMUs. Table 1 displays the experimental results.

Table 1 Experimental data for WEDM process optimization

DMU_j	Process factors				Inputs	Outputs
	A	B	C	D	$\bar{y}_{1j}$	$\bar{y}_{2j}$
DMU_1	1	1	1	1	3.15	46.00
DMU_2	1	2	2	2	3.25	47.50
DMU_3	1	3	3	3	3.30	41.50
DMU_4	2	1	2	3	3.75	55.50
DMU_5	2	2	3	1	3.45	49.50
DMU_6	2	3	1	2	3.25	52.50
DMU_7	3	1	3	2	4.10	70.50
DMU_8	3	2	1	3	3.65	73.50
DMU_9	3	3	2	1	3.35	64.00

Table 2 The center values for the three triangular membership functions

Class	Membership function center	
	c_{1d}	c_{2d}
d_q^{low}	3.15	47
d_q^{medium}	3.65	57
d_q^{High}	4.00	67

Then, the Fuzzy C-Means Clustering (FCMC) technique is used to determine the center values for the three triangular membership functions which are listed in Table 2. Each defined class is considered as a triangular membership function, whose parameters are tuned such that the center of the relative class is considered as the most likely parameter, $\bar{y}_{qd}^M$, while the centers of the neighbor classes are considered as the upper, $\bar{y}_{qd}^U$, and lower, $\bar{y}_{qd}^L$, parameters. Consequently, the experiments results shown in Table 1 are transformed into the fuzzy triangular numbers shown in Table 3.

Model 1 is used to calculate the upper efficiency values, E_j^U for all DMUs. Similarly, Model 2 is used to calculate the lower efficiency values, E_j^L for all DMUs. Model 3 is used to calculate the nominal efficiency values, E_j^U for all DMUs. Models 1, 2, and 3 are solved and the fuzzy triangular relative efficiency values are shown in Table 3.

Table 3 Fuzzy efficiency values for WEDM process optimization

DMU_j	$\check{y}_{1j}$	$\check{y}_{2j}$	$\tilde{E}_k$
DMU_1	$3.15 \approx (3.15,3.15,3.65)^{low}$	$46.0 \approx (40,47,57)^{low}$	(0.460, 0.625, 1.000)
DMU_2	$3.25 \approx (3.15,3.15,3.65)^{low}$	$47.5 \approx (40,47,57)^{low}$	(0.460, 0.625, 1.000)
DMU_3	$3.30 \approx (3.15,3.15,3.65)^{low}$	$41.5 \approx (40,47,57)^{low}$	(0.460, 0.625, 1.000)
DMU_4	$3.75 \approx (3.4,3.65,4.0)^{medium}$	$55.5 \approx (47,57,67)^{medium}$	(0.550, 0.640, 1.000)
DMU_5	$3.45 \approx (3.15,3.15,3.65)^{low}$	$49.5 \approx (40,47,57)^{low}$	(0.460, 0.625, 1.000)
DMU_6	$3.25 \approx (3.15,3.15,3.65)^{low}$	$52.5 \approx (47,57,67)^{medium}$	(0.587, 0.731, 1.000)
DMU_7	$4.1 \approx (3.65,4.2,4.2)^{high}$	$70.5 \approx (57,67,74)^{high}$	(0.555, 0.565, 1.000)
DMU_8	$3.65 \approx (3.4,3.65,3.8)^{medium}$	$73.5 \approx (57,67,74)^{high}$	(0.606, 0.752, 1.000)
DMU_9	$3.35 \approx (3.15,3.15,3.65)^{low}$	$64.0 \approx (57,67,74)^{high}$	(0.636, 0.864, 1.000)

Then, the preference degree based ranking approach is used for more clear-cut discrimination among the DMUs. Eq.(28) is used to calculate the preference matrix as shown in Table 4, where it is found that $DMU_{j=9}$ has the largest value in each column. The minimum of these nine largest values is 0.609. Hence, it is the most preferred DMU.

Table 4 Preference matrix for WEDM process optimization

DMU_j	Preference value $P(\tilde{E}_k > \tilde{E}_{j \neq k})$									Rank
	1	2	3	4	5	6	7	8	9	
DMU_1	0.500	0.500	0.500	0.461	0.500	0.357	0.458	0.306	0.227	5
DMU_2	0.500	0.500	0.500	0.461	0.500	0.357	0.458	0.306	0.227	5
DMU_3	0.500	0.500	0.500	0.461	0.500	0.357	0.458	0.306	0.227	5
DMU_4	0.539	0.539	0.539	0.500	0.539	0.383	0.491	0.327	0.240	4
DMU_5	0.500	0.500	0.500	0.461	0.500	0.357	0.458	0.306	0.227	5
DMU_6	0.643	0.643	0.643	0.617	0.643	0.500	0.589	0.435	0.328	3
DMU_7	0.542	0.542	0.542	0.509	0.542	0.411	0.500	0.359	0.359	4
DMU_8	0.694	0.694	0.694	0.673	0.694	0.565	0.640	0.500	0.390	2
DMU_9	0.773	0.773	0.773	0.759	0.773	0.672	0.719	0.609	0.500	1

3.2 Case II: Optimizing of the sputtering process parameters

Al-Refaie et al. [8] conducted eighteen experiments utilizing L_{18} array to optimize sputtering process parameters using fuzzy multiple regression based method. Five process factors considered, including: the R.F. power (P), the sputtering pressure (Q), the deposition time (R), the substrate temperature (S), and the post-annealing temperature (T). Further, three quality responses were considered including the electrical resistivity (ER), y_1, which is a STB type response, the

deposition rate (DR), y_2, which is also a STB type response and the optical transmittance (OT), y_3, which is a LTB type response. The experimental results are shown in Table 5 in term of the responses average values, $\bar{y}_{qj}$. In Table 5, the average values of ER quality response $\bar{y}_1$, are considered as inputs, while the outputs are considered as the average values of DR, $\bar{y}_2$, and OT, $\bar{y}_3$. The FCMC technique is employed to categorize each response average values into three clusters. The class center value, c_{qd} with respect to each class are calculated and listed in Table 6. The trapezoidal membership functions for all responses are shown in Table 7. Further, the fuzzy trapezoidal efficiency values and preference degree matrix for sputtering process are listed in Tables 8 and 9, respectively.

Table 5 Experimental data for sputtering process optimization

Exp. No.	Process factors					Responses		
	P	Q	R	S	T	$\bar{y}_{1j}$	$\bar{y}_{2j}$	$\bar{y}_{3j}$
1	50.00	0.13	30.00	25.00	0.00	15.10	4.60	88.40
2	50.00	0.67	60.00	50.00	100.00	9.75	5.60	87.70
3	50.00	1.33	90.00	100.00	200.00	7.85	4.95	88.10
4	100.00	0.13	30.00	50.00	100.00	5.50	9.45	89.25
5	100.00	0.67	60.00	100.00	200.00	4.45	11.20	87.05
6	100.00	1.33	90.00	25.00	0.00	6.55	10.00	84.70
7	200.00	0.13	60.00	25.00	200.00	1.65	20.00	86.60
8	200.00	0.67	90.00	50.00	0.00	1.95	21.60	82.35
9	200.00	1.33	30.00	100.00	100.00	1.70	20.90	85.45
10	50.00	0.13	90.00	100.00	100.00	7.15	4.70	87.60
11	50.00	0.67	30.00	25.00	200.00	7.00	4.95	89.10
12	50.00	1.33	60.00	50.00	0.00	7.75	4.85	87.40
13	100.0	0.13	60.00	100.00	0.00	6.00	9.70	87.00
14	100.00	0.67	90.00	25.00	100.00	5.90	11.35	83.70
15	100.00	1.33	30.00	25.00	200.00	5.60	10.75	88.35
16	200.00	0.13	90.00	50.00	200.00	1.05	19.45	83.10
17	200.00	0.67	30.00	100.00	0.00	1.25	22.05	85.70
18	200.00	1.33	60.00	25.00	100.00	1.35	20.50	83.80

Table 6 The center values for the three triangular membership functions

Class	Membership function center		
	c_{1d}	c_{2d}	c_{3d}
Low (d^{low})	1.57	4.95	83.50
Medium (d^{medium})	6.70	10.50	86.50
High (d^{high})	14.80	21.00	88.40

Table 7 Fuzzy trapezoidal experimental data for sputtering process

DMU_j	$\bar{y}_{1j}$	$\bar{y}_{2j}$	$\bar{y}_{3j}$
DMU$_1$	15.10 ≈ (6.7,14.8,15.1,15.1)^H	4.60 ≈ (4.6,4.6,4.95,10.5)^L	88.40 ≈ (86.5,88.4,90,90)^H
DMU$_2$	9.75 ≈ (6.7,14.8,15.1,15.1)^H	5.60 ≈ (4.95,9.7,11.35,21)^M	87.70 ≈ (86.5,88.4,90,90)^H
DMU$_3$	7.85 ≈ (1.57,6,7.3,14.8)^M	4.95 ≈ (4.6,4.6,4.95,10.5)^L	88.10 ≈ (86.5,88.4,90,90)^H
DMU$_4$	5.50 ≈ (1.57,6,7.3,14.8)^M	9.45 ≈ (4.95,9.7,11.35,21)^M	89.25 ≈ (86.5,88.4,90,90)^H
DMU$_5$	4.45 ≈ (1.57,6,7.3,14.8)^M	11.20 ≈ (4.95,9.7,11.35,21)^M	87.05 ≈ (86.5,88.4,90,90)^H
DMU$_6$	6.55 ≈ (1.57,6,7.3,14.8)^M	10.00 ≈ (4.95,9.7,11.35,21)^M	84.70 ≈ (83.5,86,87,88.4)^M
DMU$_7$	1.65 ≈ (1,1,1.95,5.5)^L	20.00 ≈ (10.5,19,22,22)^H	86.60 ≈ (83.5,86,87,88.4)^M
DMU$_8$	1.95 ≈ (1,1.57,1.95,6.7)^L	21.60 ≈ (12,19,22,22)^H	82.35 ≈ (82,82,83.5,86.5)^L
DMU$_9$	1.70 ≈ (1,1.57,1.95,6.7)^L	20.90 ≈ (10.5,19,22,22)^H	85.45 ≈ (83.5,86,87,88.4)^M
DMU$_{10}$	7.15 ≈ (1.57,6,7.3,14.8)^M	4.70 ≈ (4.6,4.6,4.95,10.5)^L	87.6 ≈ (83.5,86,87,88.4)^M
DMU$_{11}$	7.00 ≈ (1.57,6,7.3,14.8)^M	4.95 ≈ (4.6,4.6,4.95,10.5)^L	89.1 ≈ (86.5,88.5,90,90)^H
DMU$_{12}$	7.75 ≈ (1.57,6,7.3,14.8)^M	4.85 ≈ (4.6,4.6,4.95,10.5)^L	87.4 ≈ (86.5,88.4,90,90)^H
DMU$_{13}$	6.00 ≈ (1.57,6,7.3,14.8)^M	9.70 ≈ (4.95,9.7,11.35,21)^M	87.00 ≈ (83.5,86,87,88.4)^M
DMU$_{14}$	5.90 ≈ (1.57,6,7.3,14.8)^M	11.35 ≈ (4.95,9.7,11.35,21)^M	83.70 ≈ (82,82,83.5,86.5)^L
DMU$_{15}$	5.60 ≈ (1.57,6,7.3,14.8)^M	10.75 ≈ (4.95,9.7,11.35,21)^M	88.35 ≈ (86.5,88.5,90,90)^H
DMU$_{16}$	1.05 ≈ (1,1.57,1.95,6.7)^L	19.45 ≈ (10.5,19,22,22)^H	83.10 ≈ (82,82,83.5,86.5)^L
DMU$_{17}$	1.25 ≈ (1,1.57,1.95,6.7)^L	22.05 ≈ (10.5,19,22,22)^H	85.70 ≈ (83.5,86,87,88.4)^M
DMU$_{18}$	1.35 ≈ (1,1.57,1.95,6.7)^L	20.50 ≈ (10.5,19,22,22)^H	83.80 ≈ (82,82,83.5,86.5)^L

Table 8 Fuzzy trapezoidal efficiency values for sputtering process

DMU_j	$\tilde{E}_k$
DMU_1	(0.070,0.073,0.073,0.619)
DMU_2	(0.117,0.121,0.123,1.000)
DMU_3	0.116,0.121,0.123,1.000)
DMU_4	(0.117,0.121,0.123,1.000)
DMU_5	(0.117,0.121,0.123,1.000)
DMU_6	(0.114,0.116,0.118,1.000)
DMU_7	(0.229,0.235,0.244,1.000)
DMU_8	(0.224,0.226,0.244,1.000)
DMU_9	(0.229,0.235,0.244,1.000)
DMU_{10}	(0.114,0.116,0.117,1.000)
DMU_{11}	0.116,0.121,0.123,1.000)
DMU_{12}	(0.116,0.121,0.123,1.000)
DMU_{13}	(0.114,0.116,0.118,1.000)
DMU_{14}	(0.112,0.112,0.114,1.000)
DMU_{15}	(0.117,0.121,0.123,1.000)
DMU_{16}	(0.224,0.226,0.244,1.000)
DMU_{17}	(0.229,0.235,0.244,1.000)
DMU_{18}	(0.224,0.226,0.244,1.000)

Table 9 Preference degree matrix for the fuzzy trapezoidal efficiency values (columns 1 to 9)

	Preference value $P(\tilde{E}_k > \tilde{E}_{j \neq k})$									
	DMU_j									Rank
DMU_k	1	2	3	4	5	6	7	8	9	
DMU_1	0.500	0.320	0.320	0.320	0.320	0.324	0.207	0.212	0.207	7
DMU_2	0.680	0.500	0.500	0.500	0.500	0.504	0.403	0.407	0.403	2
DMU_3	0.679	0.499	0.50	0.499	0.499	0.503	0.402	0.406	0.402	3
DMU_4	0.680	0.500	0.500	0.500	0.500	0.504	0.403	0.407	0.403	2
DMU_5	0.680	0.500	0.500	0.500	0.500	0.504	0.403	0.407	0.403	2
DMU_6	0.676	0.495	0.495	0.495	0.495	0.500	0.400	0.404	0.400	4
DMU_7	0.792	0.595	0.596	0.595	0.595	0.598	0.500	0.504	0.500	1
DMU_8	0.641	0.393	0.394	0.393	0.393	0.398	0.495	0.500	0.495	6
DMU_9	0.792	0.595	0.596	0.595	0.595	0.598	0.500	0.504	0.500	1
DMU_{10}	0.676	0.495	0.495	0.495	0.495	0.500	0.400	0.404	0.400	4
DMU_{11}	0.679	0.499	0.50	0.499	0.499	0.503	0.402	0.406	0.402	3
DMU_{12}	0.679	0.499	0.50	0.499	0.499	0.503	0.402	0.406	0.402	3
DMU_{13}	0.676	0.495	0.495	0.495	0.495	0.500	0.400	0.404	0.400	4
DMU_{14}	0.672	0.492	0.492	0.492	0.492	0.495	0.398	0.401	0.398	5
DMU_{15}	0.680	0.500	0.500	0.500	0.500	0.504	0.403	0.407	0.403	2
DMU_{16}	0.641	0.393	0.394	0.393	0.393	0.398	0.495	0.500	0.495	6
DMU_{17}	0.792	0.595	0.596	0.595	0.595	0.598	0.500	0.504	0.500	1
DMU_{18}	0.641	0.393	0.394	0.393	0.393	0.398	0.495	0.500	0.495	6

Table 9 Preference degree matrix for the fuzzy trapezoidal efficiency values (continuation, columns 10 to 18)

	Preference value $P(\tilde{E}_k > \tilde{E}_{j \neq k})$									
	DMU_j									Rank
DMU_k	10	11	12	13	14	15	16	17	18	
DMU_1	0.324	0.320	0.320	0.324	0.327	0.320	0.212	0.207	0.212	7
DMU_2	0.504	0.500	0.500	0.504	0.506	0.500	0.407	0.403	0.407	2
DMU_3	0.503	0.500	0.500	0.503	0.503	0.499	0.406	0.402	0.406	3
DMU_4	0.504	0.500	0.500	0.504	0.506	0.500	0.407	0.403	0.407	2
DMU_5	0.504	0.500	0.500	0.504	0.506	0.500	0.407	0.403	0.407	2
DMU_6	0.500	0.495	0.495	0.500	0.502	0.495	0.404	0.400	0.404	4
DMU_7	0.598	0.596	0.596	0.598	0.601	0.595	0.792	0.595	0.596	1
DMU_8	0.398	0.394	0.394	0.398	0.398	0.393	0.500	0.495	0.500	6
DMU_9	0.598	0.596	0.596	0.598	0.601	0.595	0.792	0.595	0.596	1
DMU_{10}	0.500	0.495	0.495	0.500	0.502	0.495	0.404	0.400	0.404	4
DMU_{11}	0.503	0.500	0.500	0.503	0.503	0.499	0.406	0.402	0.406	3
DMU_{12}	0.503	0.500	0.500	0.503	0.503	0.499	0.406	0.402	0.406	3
DMU_{13}	0.500	0.495	0.495	0.500	0.502	0.495	0.404	0.400	0.404	4
DMU_{14}	0.495	0.492	0.492	0.495	0.500	0.492	0.401	0.398	0.401	5
DMU_{15}	0.504	0.500	0.500	0.504	0.506	0.500	0.407	0.403	0.407	2
DMU_{16}	0.398	0.394	0.394	0.398	0.398	0.393	0.500	0.495	0.500	6
DMU_{17}	0.598	0.596	0.596	0.598	0.601	0.595	0.792	0.595	0.596	1
DMU_{18}	0.398	0.394	0.394	0.398	0.398	0.393	0.500	0.495	0.500	6

4. Research results and discussion

4.1 Results of case I

For this case, Table 4 reveals that DMU$_9$ is the most preferred DMU. Table 10 shows the results of the proposed approach against that of the fuzzy multiple regression approach (FMRA). Using the proposed approach, the MRR fuzzy response value, $\tilde{\bar{y}}_1$, which is a LTB type response improved from (56.4, 59.10, 62.46) to (57, 67, 74), where the $\bar{y}_2^U$ and $\bar{y}_2^M$ values are significantly increased. Also, the SR fuzzy response value, $\tilde{\bar{y}}_2$, which is a STB type response improves from (2.94, 3.32, 3.75) to (3.15, 3.15, 3.65). Note that the proposed approach provides smaller mean and upper bound value than FMRA. Therefore, to improve the performance of WEDM process, the best combination of factor settings is pulse in time A_3, delay time B_3, wire feed speed C_2, ignition current D_1.

Table 10 Improvement comparison for case I

Response	$\tilde{\bar{y}}_1$ (LTB)	$\tilde{\bar{y}}_2$ (STB)
Initial condition	≈ (49.4,51.9,54.58)	≈ (2.99,3.42,3.92)
Fuzzy multiple regression approach (FMRA)	≈ (56.4,59.10,62.46)	≈ (2.94,3.32,3.75)
Proposed approach results (IDEA)	≈ (57,67,74)	≈ (3.15,3.15,3.65)

4.2 Results for case II

For case II, it is found that DMU$_9$ is the best DMU, which corresponds as shown in Table 5. Table 11 displays the anticipated improvements using the proposed approach and FMRA.

Using the proposed approach the fuzzy trapezoidal value of the ER, $\bar{y}_1$, which is a STB type response decreased from (1.39, 2.91, 3.19, 4.32) to (1.0, 1.57, 1.95, 6.7). Although the proposed approach increased the upper response value, $\bar{y}_1^U$ it significantly decreased the lower mid and upper mid response values. For DR, $\bar{y}_2$, which is a LTB type response, the proposed approach enhances the response fuzzy trapezoidal value from (11.84, 12.26, 12.75 21.94) to (10.5, 19, 21, 22). Finally for OT, $\bar{y}_3$, which is a LTB type response, the proposed approach improves the upper response value from 87.7 to 88.5. Consequently, the best combination of factor settings for the sputtering process is the R.F. power $P = 200$, the sputtering pressure $Q = 1.33$, the deposition time $R = 30$, the substrate temperature $S = 100$, and the post-annealing temperature $T = 100$.

Table 11 Improvement comparison for case II

Methods	Quality responses											
	y_1 (STB, input)				y_2 (LTB, output)				y_3 (LTB, output)			
	y_1^L	y_1^{ML}	y_1^{UL}	y_1^U	y_2^L	y_2^{ML}	y_2^{UL}	y_2^U	y_3^L	y_3^{ML}	y_3^{UL}	y_3^U
FMRA results	1.39	2.91	3.19	4.32	11.84	12.26	12.75	21.94	86.4	86.5	87.6	87.7
IDEA results	1.0	1.57	1.95	6.7	10.5	19.0	21.0	22.0	83.5	86.0	87.0	88.5

5. Conclusions

In this research, a fuzzy DEA based procedure is proposed to solve the fuzzy multiple responses problem in robust design. DEA models are utilized to calculate the fuzzy efficiencies. Then, the preference matrix is adopted to identify the best decision making unit. Two real case studies from previous literature are employed to illustrate the proposed approach including improving performance of the WEDM and sputtering processes, where the response fuzziness is fitted by a triangular and trapezoidal membership functions in the first and second case study, respectively. In both studies, the proposed approach efficiently identified the best combination of factor settings and provides better anticipated improvements than the fuzzy multiple regression based approach. In conclusion, the proposed approach may provide great assistant to process engineers in determining the best combination of factor settings that improves fuzzy multiple re-

sponses in a wide range of business applications. Nevertheless, this approach ignores process factor settings and preferences on quality responses. Another limitation is its complexity when many fuzzy responses are considered simultaneously. Future research will consider these issues.

References

[1] Liao, H.-C., Chen, Y.-K. (2002). Optimizing multi-response problem in the Taguchi method by DEA based ranking approach, *International Journal of Quality & Reliability Management*, Vol. 19, No.7, 825-837, doi: 10.1108/02 656710210434766.
[2] Reddy, P.B.S, Nishina, K., Babu A.S. (1997). Unification of robust design and goal programming for multiresponse optimization – a case study, *Quality and Reliability Engineering International*, Vol. 13, No. 6, 371-383.
[3] Hsu, C.-M. (2001). Solving multi-response problems through neural networks and principal component analysis, *Journal of the Chinese Institute of Industrial Engineers*, Vol. 18, No. 5, 47-54, doi: 10.1080/10170660109509504.
[4] Salmasnia, A., Kazemzadeh, R.B., Niaki, S.T.A. (2012). An approach to optimize correlated multiple responses using principal component analysis and desirability function, *The International Journal of Advanced Manufacturing Technology*, Vol. 62, No. 5-8, 835-846, doi: 10.1007/s00170-011-3824-2.
[5] Al-Refaie, A. (2012). Optimizing performance with multiple responses using cross-evaluation and aggressive formulation in data envelopment analysis, *IIE Transactions*, Vol. 44, No. 4, 262-276, doi: 10.1080/0740817X. 2011.566908.
[6] Al-Refaie, A., Wu, T.-H, and Li, M.-H. (2009). Data envelopment analysis approaches for solving the multiresponse problem in the Taguchi method, *Artificial Intelligence for Engineering Design, Analysis and Manufacturing*, Vol. 23, No. 2, 159-173, doi: 10.1017/S0890060409000043.
[7] Al-Refaie, A. (2010). Grey-data envelopment analysis approach for solving the multi-response problem in the Taguchi method, In: *Proceedings of the Institution of Mechanical Engineers, Part B: Journal of Engineering Manufacture*, Vol. 224, No. 1, 147-158, doi: 10.1243/09544054JEM1525.
[8] Al-Refaie, A., Rawabdeh, I., Abu-alhaj, R., Jalham, I.S. (2012). A fuzzy multiple regressions approach for optimizing multiple responses in the Taguchi method, *International Journal of Fuzzy System Applications*, Vol. 2, No. 3, 13-34, doi: 10.4018/ijfsa.2012070102.
[9] Hsieh, K.-L., Tong, L.-I. (2001). Optimization of multiple quality responses involving qualitative and quantitative characteristics in IC manufacturing using neural network, *Computers in Industry*, Vol. 46, No. 1, 1-12, doi: 10.1016/S0166-3615(01)00091-4.
[10] Al-Refaie, A., Li, M.-H. (2011). Optimizing the performance of plastic injection molding using weighted additive model in goal programming, *International Journal of Fuzzy System Applications*, Vol. 1, No. 2, 43-54, doi: 10.4018/ ijfsa.2011040104.
[11] Kim, K., Lin, D. (2000). Simultaneous optimization of multiple responses by maximizing exponential desirability functions, *Journal of the Royal Statistical Society: Series C (Applied Statistics)*, Vol. 49, No. 3, 311-325.
[12] Kim, K.-J., Lin, D.K.J. (2006). Optimization of multiple responses considering both location and dispersion effects, *European Journal of Operational Research*, Vol. 169, No. 1, 133-145, doi: 10.1016/j.ejor.2004.06.020.
[13] Fung, C.-P., Kang, P.-C. (2005). Multi-response optimization in friction properties of PBT composites using Taguchi method and principle component analysis, *Journal of Materials Processing Technology*, Vol. 170, No. 3, 602-610, doi: 10.1016/j.jmatprotec.2005.06.040.
[14] Khalili-Damghani, K., Taghavifard, M., Olfat, L., Feizi, K. (2011). A hybrid approach based on fuzzy DEA and simulation to measure the efficiency of agility in supply chain: real case of dairy industry, *International Journal of Management Science and Engineering Management*, Vol. 6, No. 3, 163-172.
[15] Zhu, J. (2003). Imprecise data envelopment analysis (IDEA): A review and improvement with an application, *European Journal of Operational Research*, Vol. 144, No. 3, 513-529, doi: 10.1016/S0377-2217(01)00392-7.
[16] Shokouhi, A.H., Shahriari, H., Agrell, P.J., Hatami-Marbini, A. (2014). Consistent and robust ranking in imprecise data envelopment analysis under perturbations of random subsets of data, *OR Spectrum*, Vol. 36, No. 1, 133-160, doi: 10.1007/s00291-013-0336-5.
[17] Jahanshahloo, G.R., Abbasian-Naghneh, S. (2011). Data envelopment analysis with imprecise data, *Applied Mathematical Sciences*, Vol. 5, No. 62, 3089-3106.
[18] Wang, Y.-M., Luo, Y., Liang, L. (2009). Fuzzy data envelopment analysis based upon fuzzy arithmetic with an application to performance assessment of manufacturing enterprises, *Expert Systems with Applications*, Vol. 36, No. 3(Part 1), 5205-5211, doi: 10.1016/j.eswa.2008.06.102.

Hybrid Taguchi method for optimizing flux cored arc weld parameters for mild steel

Satheesh, M.[a], **Edwin Raja Dhas, J.**[b,*]

[a]Department of Mechanical Engineering, Noorul Islam Centre for Higher Education, Kumaracoil, Thuckalay, India
[b]Department of Automobile Engineering, Noorul Islam Centre for Higher Education, Kumaracoil, Thuckalay, India

A B S T R A C T

Flux cored arc welding has been applied in manufacturing industries for more than fifteen years. The quality of weld mainly depends on the mechanical properties of the weld, which in turn relays on the interaction of the weld parameters. This paper discusses the multi response optimization of weld parameters using grey based Taguchi method. Grey relational analysis was carried out to convert multi objective criterion into equivalent single objective function; overall grey relational grade, which is optimized by the Taguchi technique. Experiments are conducted using Taguchi's L_{27} orthogonal array. The weld parameters used in this study were welding current, welding speed, and arc voltage with bead hardness and material deposition rate as responses. Taguchi's Signal-to-Noise (S/N) ratio is computed based on their performance characteristics. Grey relational grade was obtained using Signal-to-Noise ratio values of responses. Based on the grey relational grade, optimum levels of parameters have been identified. Significant contributions were estimated using Analysis of Variance (ANOVA). A confirmation test was conducted to validate the proposed method. This evaluation procedure could be used in decision-making to select process parameters for a welding operator. The proposed and developed method has good accuracy and competency with the predicted value enhancing automation and robotization.

1. Introduction

Generally, the quality of a weld joint is directly influenced by the welding input parameters during the welding process; therefore, welding can be considered as a multi-input multi-output process. Unfortunately, a common problem that has faced the manufacturer is the control of the process input parameters to obtain a good welded joint with the required bead geometry and weld quality with maximum deposition rate. Weld deposition rate is the weight (in kg) of weld metal deposited per unit of arc-on-time (usually one hour). The weight deposited is less than the weight of the filler metal used, because of various losses. The ratio of the weight of metal deposited in the weld to that of filler metal employed, expressed in percent, is called the deposition efficiency. Flux cored arc welding process is a fully automated process, in which the welding electrode is a tubular wire that is continuously fed to the weld area [1]. The flux materials are in the core of the tube. The outer shell of the tube conducts the electricity that forms the arc and then becomes the filler metal as it is consumed. Recent studies indicate that FCAW has a number of advantages over the common welding techniques available that use solid wires such as manual metal arc welding and gas metal arc welding [2]. Using FCAW in any repair technique can pro-

vide better control over current and heat input that is necessary to carry out the temper bead repair. As a fully automatic process, FCAW should also have cost advantages over other commonly used processes. Flux cored arc welding is considered a high deposition rate welding process that adds the benefits of flux to the simplicity of metal inert gas welding [3]. Many research attempts have been made by researchers to establish flux cored arc welding process. Mathematical modeling [4], particle swarm optimization algorithm [5], simulated annealing algorithm [6], memetic algorithm [7], Taguchi method [8], were used to optimize the parameters of flux cored arc welding process. Traditional Taguchi method can optimize a single objective function whereas it cannot solve multi objective function [9]. This paper explores the development of grey based Taguchi method for multi response optimization of flux cored arc weld parameters.

2. Grey based Taguchi method

To resolve the problems subjected to multiple quality characteristics, a decision maker should rely on the subjective experiences of engineers to attain a compromise. As a result, uncertainty will be increased during the process. Hence some researchers have concentrated on achieving multiple quality characteristic at a time as a function of different appropriate level of input parameter settings. Orthogonal array with principle component analysis and Taguchi method and response surface methodology applied [10, 11] to optimize multiple quality characteristics during laser cutting of different thin sheets. Fuzzy based desirability function is used to optimize parameters of weld [12].

Grey relational analysis aims to fulfil the crucial mathematical criteria for multiple quality characteristic problems [13]. It avoids the inherent shortcomings of conventional, statistical methods and requires a limited data to estimate the behavior of an uncertain system. It provides an efficient solution to the uncertain, multi-input and discrete data problem. The main function of Grey relational analysis is to indicate the relational degree between two sequences by using discrete measurement method the distance. It can be effectively recommended as a method for optimizing the complicated interrelationships among multiple performance characteristics.

2.1 Taguchi method

The quality engineering methods of Taguchi, employing design of experiments provide an efficient and systematic way to optimize designs for performance, quality and cost. It is one of the most important statistical tools for designing high quality systems at reduced cost [14, 15]. The use of Taguchi method simplifies the optimization procedure for determining the optimal welding parameters in the FCAW process. The Taguchi method is performed to reduce the sources of variation on the quality characteristics of product, and reach a target of process robustness. The control factors that may contribute to reduce variation (improved quality) can be quickly identified by looking at the amount of variation present as a response. Taguchi recommends the use of the loss function to measure the performance characteristic deviating from the desired value. The value of the loss function is then transformed into an S/N ratio. Usually, there are three categories [16] of performance characteristic in the analysis of the S/N ratio, i.e. lower-the-better, higher-the-better, and nominal-the-best. The deposition rate and hardness are the higher the better performance characteristic. The S/N ratio η_{ij} for the ith performance characteristic in the jth experiment can be expressed as Eq. 1.

$$\eta_{ij} = -10\log(L_{ij}) \qquad (1)$$

The loss function L_{ij} for higher-the-better performance characteristic is expressed in Eq. 2:

$$L_{ij} = \frac{1}{n}\sum_{k=1}^{n}\frac{1}{y_{ijk}^2} \qquad (2)$$

where n is the number of replication, k is the number of tests, y_{ijk} is experimental value of the ith performance characteristic in the jth experiment at the kth tests.

For lower-the-better performance characteristic, L_{ij} is expressed in Eq. 3.

$$L_{ij} = \frac{1}{n} \sum_{k=1}^{n} y_{ijk}^2 \qquad (3)$$

For nominal-is-best performance characteristics, the S/N ratio is expressed in Eq. 4.

$$\eta_{ij} = 10\log\left(\frac{\bar{y}}{\sigma}\right) \qquad (4)$$

The S/N ratio for each level of process parameters is computed based on the S/N analysis. This S/N ratio value can be considered for the optimization of single response problems. However, optimization of multiple performance characteristics cannot be straightforward as in the optimization of a single performance characteristic.

2.2 Grey relational analysis

The grey relational analysis is based on the grey system theory used to solve complicated inter-relationship multiple performance characteristics problems effectively. A grey system has a level of information between black and white. Black represents having no information and white represents having all information. Grey based Taguchi method is successfully applied to optimize film coating process [17], drilling process [18], plasma arc weld parameters [19], bead geometry in SAW process, and wire electrical discharge machining process [20, 21].

Depending upon the characteristics of a data sequence, there are various methodologies of data pre-processing available for this analysis. Experimental data y_{ij} is normalized as Z_{ij} $(0 \le Z_{ij} \le 1)$ for the ith performance characteristics in the jth experiment is expressed as:

For S/N ratio with larger-the-better:

$$Z_{ij} = \frac{y_{ij} - min(y_{ij}, i = 1,2, \dots, n)}{max(y_{ij}, i = 1,2, \dots, n) - min(y_{ij}, i = 1,2, \dots, n)} \qquad (5)$$

For S/N ratio with smaller-the-better:

$$Z_{ij} = \frac{max(y_{ij}, i = 1,2, \dots, n)}{max(y_{ij}, i = 1,2, \dots, n) - min(y_{ij}, i = 1,2, \dots, n)} \qquad (6)$$

For S/N ratio with nominal-the-best:

$$Z_{ij} = \frac{(y_{ij} - \text{Target}) - min(|y_{ij} - \text{Target}|, i = 1,2, \dots, n)}{max(|y_{ij} - \text{Target}|, i = 1,2, \dots, n) - min(|y_{ij} - \text{Target}|, i = 1,2, \dots, n)} \qquad (7)$$

Then, the grey relational coefficients are calculated to express the relationship between the ideal and the actual experimental results. The grey relational co-efficient is expressed in Eq. 8:

$$\gamma_{ij} = \frac{\Delta min + \xi \Delta max}{\Delta_{oj}(k) + \xi \Delta max} \qquad (8)$$

where $j = 1, 2, \dots, n$, $k = 1, 2, \dots, m$, n is the number of experimental data items, and m is the number of responses. $y_o(k)$ is the reference sequence $y_o(k) = 1$, $k = 1, 2, \dots, m$, and $y_j(k)$ is the specific comparison sequence.

The absolute value of the difference between $y_o(k)$ and $y_j(k)$:

$$\Delta_{oj} = \|y_o(k) - y_i(k)\| \tag{9}$$

Δ_{min} is the smallest value of $y_j(k)$:

$$\Delta_{min} = \min_{\forall j \in i} \min_{\forall k} \|y_o(k) - y_i(k)\| \tag{10}$$

Δ_{max} is the largest value of $y_j(k)$:

$$\Delta_{max} = \max_{\forall j \in i} \max_{\forall k} \|y_o(k) - y_i(k)\| \tag{11}$$

ξ is the distinguishing coefficient which is defined in the range 0 to 1 (the value is adjusted based on the practical needs of the system)

The Grey relational grade is expressed in Eq. 12:

$$\bar{\gamma}_j = \frac{1}{k} \sum_{i=1}^{m} y_{ij} \tag{12}$$

where j is the grey relational grade for the jth experiment and k is the number of performance characteristics. Higher grey relational grade implies the better product quality, therefore, on the basis of grey relational grade, the factor effect is estimated using ANOVA [23] and the optimal level for each controllable factor is determined.

3. Experimental work

Experiments are conducted using SUPRA INVMIG 500 welding machine using DC electrode positive (DCEP). Test pieces of size 200 mm × 150 mm × 6 mm are cut from low carbon structural steel (IS: 2062) plate and its surfaces are ground to remove oxide scale and dirt before cladding. Flux cored mild steel electrode (E71T-1) of 1.2 mm diameter is used for welding. CO_2 gas at a constant flow rate of 15 L/min is used for shielding. The experimental setup used consists of a traveling carriage with a table for supporting the specimens. The welding torch is held stationary in a frame mounted above the work table, and it is provided with an attachment for both up and down movement and angular movement for setting the required nozzle-to-plate distance and welding torch angle, respectively. Single pass welding bead on joint weld with square butt weld is performed on the weld plates by varying the initial parameters as shown in Table 1. The working ranges for the process parameters are selected from the American Society Welding handbook [24]. Each trial of experiment was done twice and the average value is taken.

Deposition rate and hardness are considered as objectives. The metal deposition rate is calculated with the help of stop watch and length of the electrode melt during the welding process. Brinnel hardness test is performed using Brinnel hardness testing machine. Based on the designed orthogonal array combination a series of joining processes are performed in welding machine. Experimental results are summarized in Table 2.

Table 1 Welding Parameters and their levels

Factors	Welding parameters	Level 1	Level 2	Level 3
I	Welding current (A)	180	220	260
V	Arc voltage (V)	20	24	28
S	Electrode stick-out (mm)	19	21	24

Table 2 Experimental results for hardness and deposition rate

Exp. No.	I	V	S	Hardness (HB)	Deposition rate (kg/h)
1	1	1	1	320.96	2.12
2	1	1	2	496.41	2.15
3	1	1	3	469.83	2.21
4	1	2	1	465.45	1.48
5	1	2	2	589.83	1.92
6	1	2	3	519.96	2.21
7	1	3	1	433.83	1.44
8	1	3	2	580.99	1.48
9	1	3	3	519.83	2.16
10	2	1	1	329.96	2.58
11	2	1	2	259.83	5.26
12	2	1	3	445.07	2.86
13	2	2	1	449.96	2.45
14	2	2	2	595.07	2.01
15	2	2	3	265.07	5.61
16	2	3	1	389.96	2.37
17	2	3	2	549.96	2.31
18	2	3	3	459.83	2.26
19	3	1	1	269.96	4.08
20	3	1	2	485.09	3.39
21	3	1	3	345.09	4.32
22	3	2	1	424.15	3.01
23	3	2	2	515.09	3.75
24	3	2	3	488.41	3.83
25	3	3	1	319.96	3.97
26	3	3	2	464.15	4.18
27	3	3	3	449.83	3.71

4. Results and discussion

S/N ratios for deposition rate and hardness are computed using Eq. 1, Eq. 2, and Eq. 3. Using Eq. 5 and Eq. 6 the S/N ratios are normalized and shown in Table 3. Grey relational coefficient for each performance characteristic is calculated using Eq. 8. The value for ξ is taken as 0.5 since both the process parameters are of equal importance. The grey relational grade is calculated using Eq. 12, which is the overall representative of both the responses shown in Table 4.

Now, the multiple objective optimization problems have been transformed into a single equivalent objective function optimization problem using this approach. The higher grey relational grade is said to be close to the optimal. The mean response table for overall grey relational grade is shown in Table 5 and is represented graphically in Fig 1. With the help of the response table and response graph, the optimal parameter combination has been determined as $I_1V_3S_3$.

Using the grey relational grade value, ANOVA is formulated for identifying the significant factors. The results of ANOVA are presented in Table 6. From ANOVA, it is clear that welding speed (64.42 %) influences more on welding of mild steel plates followed by arc voltage (18.54 %) and welding current (1.07 %).

In order to predict the optimum condition, the expected mean at the optimal settings (μ) is calculated by using the following model $\mu = \bar{I}_1 + \bar{V}_3 + \bar{S}_3 - 2 \cdot \bar{T}_{gg}$, where $\bar{I}_1$, $\bar{V}_3$, and $\bar{S}_3$ are the mean values of the grey relational grade with the parameters at optimum levels, and $\bar{T}_{gg}$ is the overall mean of average grey grade. The expected mean (μ) at optimal setting is found to be 0.5950.

Table 3 S/N ratios and their normalize values

Exp. No.	S/N ratio		Normalized values of S/N ratio	
	Hardness (HB)	Deposition rate (kg/h)	Hardness (HB)	Deposition rate (kg/h)
1	50.129	6.5267	0.1823	0.1631
2	53.9168	6.6488	0.7057	0.1703
3	53.4388	6.8878	0.6264	0.1847
4	53.3575	3.4052	0.6134	0.0096
5	55.4145	5.666	0.9844	0.1151
6	54.3194	6.8878	0.776	0.1847
7	52.7464	3.1672	0.519	0
8	55.2834	3.4052	0.958	0.0096
9	54.3172	6.6891	0.7756	0.1727
10	50.3692	8.2324	0.2092	0.2734
11	48.2938	14.4197	0	0.9161
12	52.9686	9.1273	0.5526	0.3405
13	53.0635	7.7833	0.5671	0.2422
14	55.4914	6.0639	1	0.1367
15	48.4672	14.9793	0.0156	1
16	51.8204	7.495	0.3882	0.223
17	54.8066	7.2722	0.8654	0.2086
18	53.2519	7.0822	0.5966	0.1966
19	48.626	12.2132	0.0302	0.6331
20	53.7164	10.604	0.6719	0.4676
21	50.7586	12.7097	0.2543	0.6906
22	52.5504	9.5713	0.4902	0.3765
23	54.2377	11.4806	0.7614	0.554
24	53.7757	11.664	0.6818	0.5731
25	50.1019	11.9758	0.1794	0.6067
26	53.3332	12.4235	0.6095	0.6571
27	53.061	11.3875	0.5668	0.5444

Table 4 Grey relational coefficients of responses

Exp. No.	S/N ratio		Grey relational grade
	Hardness (HB)	Deposition rate (kg/h)	
1	0.3795	0.374	0.3767
2	0.6295	0.376	0.5028
3	0.5724	0.3801	0.4762
4	0.5639	0.3355	0.4497
5	0.9697	0.361	0.6654
6	0.6906	0.3801	0.5353
7	0.5097	0.3333	0.4215
8	0.9225	0.3355	0.629
9	0.6902	0.3767	0.5334
10	0.3874	0.4076	0.3975
11	0.3333	0.8563	0.5948
12	0.5277	0.4312	0.4795
13	0.536	0.3975	0.4668
14	1	0.3668	0.6834
15	0.3368	1	0.6684
16	0.4497	0.3915	0.4206
17	0.7879	0.3872	0.5876
18	0.5535	0.3836	0.4685
19	0.3402	0.5768	0.4585
20	0.6038	0.4843	0.5441
21	0.4014	0.6178	0.5096
22	0.4951	0.445	0.4701
23	0.677	0.5285	0.6027
24	0.6111	0.5395	0.5753
25	0.3786	0.5597	0.4692
26	0.5615	0.5932	0.5773
27	0.5358	0.5232	0.5295

Table 5 Response table for overall grey relational grade

Factors	Level 1	Level 2	Level 3
I	0.51	0.4821	0.4367
V	0.5296	0.5685	0.5985
S	0.5262	0.5151	0.5306

Table 6 Response table for overall grey relational grade

| Factors	Degrees of freedom	Sum of squares	Mean squares	F value	Contribution (%)
I	2	0.00198	0.000993	0.68	1.07
V	2	0.0342	0.017102	11.65	18.54
S	2	0.1188	0.05943	40.47	64.42
Error	20	0.0293	0.00146		15.88
Total	26	0.18441			100
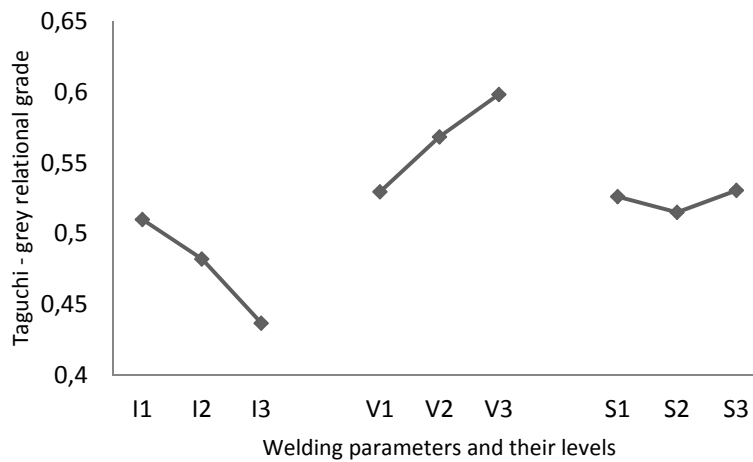
Fig. 1 Response graph for grey relational grade

Once the optimal level of the process parameters has been determined, the final step is to predict and verify the improvement of the performance characteristic using the optimal level of weld parameters. Table 7 shows the comparison of the multiple performance characteristics for initial and optimal welding parameters. The initial designated levels of welding parameters are I2, V1, and S3. As noted from Table 7, the deposition rate is increased from 2.06 kg/h to 2.16 kg/h and the hardness is increased from 480.31 to 519.83. The estimated grey relational grade is increased from 0.4818 to 0.5334. It is clearly shown that the multiple objectives of the weld process are together improved remarkably.

Table 7 Results of initial and optimal welding performance

	Initial process parameters	Optimal process parameters	
		Prediction	Experiment
Level	$I_2V_1S_3$	$I_1V_3S_3$	$I_1V_3S_3$
Hardness	480.31		519.83
Deposition rate	2.06		2.16
Grey relational grade	0.4818	0.595	0.5334
Improvement of Grey relational grade		0.1132	0.0516

5. Conclusion

Effects of welding parameters and the optimum welding parameters for a FCAW process on the multiple performance characteristics are systematically investigated by Taguchi-based grey relational analysis. Application of Taguchi optimization technique coupled with grey relational analysis has been adopted for estimating the optimal parametric combination to achieve ac-

ceptable (maximum) bead hardness and deposition rate. Signal-to-Noise ratio is computed based on their performance characteristics.

Grey relational grade is obtained using Signal-to-Noise ratio values of responses. Based on grey relational grade, optimum levels of parameters have been identified. The significant contributions are estimated using analysis of variance. It is found that electrode stick out (64.42 %) influences more followed by arc voltage (18.57 %) and welding current (1.07 %). The best performance characteristics is obtained with lower welding current of 180 A, higher arc voltage of 28 V and higher electrode stick out of 24 mm. Confirmatory experiments prove that the determined optimal conditions of weld parameters to satisfy real conditions. The proposed and developed algorithm simplifies the optimization design of weld parameters with multiple-performance characteristics. Thus, the solutions from this method can be used by engineers willing to search for any weld optimal solution.

Acknowledgement

References

[1] Aloraier, A., Ibrahim, R., Thomson, P. (2006). FCAW process to avoid the use of post weld heat treatment, *International Journal of Pressure Vessels and Piping*, Vol. 83, No. 5, 394-398, doi: 10.1016/j.ijpvp.2006.02.028.
[2] Parmar, R.S. (1999). *Welding processes and technology*, Khanna Publishers, New Delhi.
[3] Murugan, N., Parmar, R.S. (1994). Effects of MIG process parameters on the geometry of the bead in the automatic surfacing of stainless steel, *Journal of Materials Processing Technology*, Vol. 41, No. 4, 381-398, doi: 10.1016/0924-0136(94)90003-5.
[4] Raveendra, J., Parmar, R.S. (1987). Mathematical models to predict weld bead geometry for flux cored arc welding, *Journal of Metal Construction*, Vol. 19, No. 2, 31-35.
[5] Katherasan, D., Elias, J.V., Sathiya, P., Noorul Haq, A. (2012). Flux cored arc welding parameter optimization using particle swarm optimization algorithm, *Procedia Engineering*, Vol. 38, 3913-3926, doi: 10.1016/j.proeng. 2012. 06.449.
[6] Katherasan, D., Elias, J.V., Sathiya, P., Noorul Haq, A. (2013). Modeling and optimization of flux cored arc welding by genetic algorithm and simulated annealing algorithm, *Multidiscipline Modeling in Materials and Structures*, Vol. 9, No. 3, 307-326, doi: 10.1108/MMMS-03-2012-0008.
[7] Kannan, T., Murugan, N., Sreeharan, B.N. (2013). Optimization of flux cored arc welding process parameter using genetic and memetic algorithms, *Journal for Manufacturing Science and Production*, Vol. 13, No. 4, 239-250, doi: 10.1515/jmsp-2012-0040.
[8] Biswas, B.K., Bandyopadhyay, A., Pal, P.K. (2014). A study on quality of weld in flux cored arc welding process, *International Journal of Precision Technology*, Vol. 4, No. 1/2, 81-95, doi: 10.1504/IJPTECH.2014.060619.
[9] Moshat, S., Datta, S., Bandyopadhyay, A., Pal, P. (2010). Optimization of CNC end milling process parameters using PCA-based Taguchi method, *International Journal of Engineering, Science and Technology*, Vol. 2, No. 1, 92-102.
[10] Liao, H.-C. (2006). Multi-response optimization using weighted principal component, *The International Journal of Advanced Manufacturing Technology*, Vol. 27, No. 7-8, 720-725 doi: 10.1007/s00170-004-2248-7.
[11] Gunaraj, V., Murugan, N. (1999). Application of response surface methodology for predicting weld bead quality in submerged arc welding of pipes, *Journal of Materials Processing Technology*, Vol. 88, No. 1-3, 266-275, doi: 10.1016/S0924-0136(98)00405-1.
[12] Satheesh, M., Edwin Raja Dhas, J. (2014). Multi objective optimization of weld parameters of boiler steel using fuzzy based desirability function, *Journal of Engineering Science and Technology Review*, Vol. 7, No. 1, 29-36.
[13] Jeyapaul, R., Shahabudeen, P., Krishnaiah, K. (2005). Quality management research by considering multi-response problems in the Taguchi method – a review, *The International Journal of Advanced Manufacturing Technolgy*, Vol. 26, No. 11-12, 1331-1337, doi: 10.1007/s00170-004-2102-y.
[14] Taguchi, G. (1986). *Introduction to quality engineering: designing quality into products and processes*, Asian Productivity Organization, Tokyo, Japan.
[15] Peace, G.S. (1992). *Taguchi methods: a hands-on approach*, Addison-Wesley, Massachusetts, USA.
[16] Kumanan, S., Edwin Raja Dhas, J., Gowthaman, K. (2007). Determination of submerged arc welding process prameters using Taguchi method and regression analysis, *Indian Journal of Engineering & Materials Sciences*, Vol. 14, 177-183.
[17] Kuo, C.-F.J., Wu, Y.-S. (2006). Optimization of the film coating process for polymer blends by the grey-based Taguchi method, *The International Journal of Advanced Manufacturing Technology*, Vol. 27, No. 5-6, 525-530, doi: 10.1007/s00170-004-2217-1.

[18] Tosun, N. (2006). Determination of optimum parameters for multi-performance characteristics in drilling by using grey relational analysis, *The International Journal of Advanced Manufacturing Technology*, Vol. 28, No. 5-6, 450-455, <u>doi: 10.1007/s00170-004-2386-y</u>.

[19] Hsiao, Y.F., Tarng, Y.S., Huang, W.J. (2007).Optimization of plasma arc welding parameters by using the Taguchi method with the grey relational analysis, *Materials and Manufacturing Processes*, Vol. 23, No. 1, 51-58, <u>doi: 10.1080/10426910701524527</u>.

[20] Kamal, J., Ajai, J., Sandeep, G. (2010). Optimization of multiple-machining characteristics in wire electrical discharge machining of punching die using Grey relational analysis, *Journal of Scientific and Industrial Research*, Vol. 69, No. 8, 606-612.

[21] Muthu Kumar, V., Suresh Babu, A., Venkatasamy, R., Raajenthiren, M. (2010). Optimization of the WEDM parameters on machining Incoloy800 super alloy with multiple quality characteristics, *International Journal of Engineering Science and Technology*, Vol. 2, No. 6, 1538-1547.

[22] Balasubramanian, S., Ganapathy, S. (2011). Grey relational analysis to determine optimum process parameters for wire electro discharge machining (WEDM), *International Journal of Engineering Science and Technology*, Vol. 3, No. 1, 95-101.

[23] Fisher, R.A. (1970). *Statistical methods for research workers*, Oliver and Boyd, Edinburgh, United Kingdom.

Calendar of events

- The 9th ASME International Manufacturing Science and Engineering Conference (MSEC 2014); 42nd North American Manufacturing Research Conference (NAMRC 42); JSME International Conference on Materials and Processing (ICM&P 2014), Detroit, USA, June 9-13, 2014.
- Manufacturing Process Excellence Conference, Chicago, Illinois, USA, June 16-18, 2014.
- 6th International Conference on Tribology in Manufacturing Processes & Joining by Plastic Deformation (ICTMP 2014), Darmstadt, Germany, June 22-24, 2014.
- International Conference on Mechanical Engineering and Industrial Manufacturing (CMEIM 2014), Nanjing, China, June 27-29, 2014.
- International Conference on Robotics and Mechatronics (ICROM 2014), Nottingham, United Kingdom, July 6-7, 2014.
- 2nd CIRP Conference on Robust Manufacturing (RoMaC 2014), Bremen, Germany, July 7-9, 2014.
- 9th International Conference on Additive Manufacturing and 3D Printing, Nottingham, United Kingdom, July 7-11, 2014.
- 27th International CADCAM, Robotics and Factories of the Future, July 22-24, 2014, London, United Kingdom.
- 9th CIRP Conference on Intelligent Computation in Manufacturing Engineering (CIRP IC-ME'14), Capri (Naples), Italy, July 23-25, 2014.
- 2nd Journal Conference on Modeling and Optimization (JCMO 2014), Hong Kong, China, July 28-29, 2014.
- 2nd International Conference on Industrial and Production Engineering (ICIPE 2014), Chengdu, Kuala Lumpur, Malaysia, September 2-3, 2014.
- International Conference on Mechatronics, Materials and Manufacturing (ICMMM 2014), Chengdu, China, August 2-4, 2014.
- International Conference on Manufacturing and Optimization (ICMO 2014), Chengdu, China, September 6-8, 2014.
- 11th International Conference on High Speed Machining, Advances in Manufacturing Technology (HSM 2014), Prague, Czech Republic, September 11-12, 2014.
- The 4th International Conference on Industrial Technology and Management (ICITM 2014), Paris, France, September 17-18, 2014.
- 15th International Conference MetalForming 2014, Palermo, Italy, September 21-24, 2014.
- 12th Global Conference on Sustainable Manufacturing (GCSM), Malaysia, September 22-24, 2014.
- 3rd Journal Conference on Innovation, Management and Technology (JCIMT 2014), Geneva, Switzerland , October 10-11, 2014.
- The 15th Asia Pacific Industrial Engineering and Management Systems Conference (APIEMS 2014), Jeju, Republic of Korea, October 12-15, 2014.
- 44th International Conference on Computers & Industrial Engineering (CIE'44), Istanbul, Turkey, October 14-16, 2014.
- 22nd International Conference on Materials and Technology, Portoroz, Slovenia, October 20-22, 2014.
- International Conference on Mechatronics, Automation and Manufacturing (ICMAM 2014), Beijing, China, October 24-26, 2014.
- International Conference on Mechatronics and Intelligent Manufacturing (ICMIM 2014), Bahrain, Bahrain, November 5-7, 2014.
- 25th DAAAM International Symposium on Intelligent Manufacturing and Automation, Vienna, Austria, November 26-29, 2014.
- IEEE International Conference on Industrial Technology, Seville, Spain, March 17-19, 2015.
- IEEE International Conference on Robotics and Automation, Seattle, Washington, USA, May 25-30, 2015.

Notes for contributors

General

Articles submitted to the *APEM journal* should be original and unpublished contributions and should not be under consideration for any other publication at the same time. Extended versions of articles presented at conferences may also be submitted for possible publication. Manuscript should be written in English. Responsibility for the contents of the paper rests upon the authors and not upon the editors or the publisher. Authors of submitted papers automatically accept a copyright transfer to *Production Engineering Institute*, *University of Maribor*.

Submission of papers

A submission must include the corresponding author's complete name, affiliation, address, phone and fax numbers, and e-mail address. All papers for consideration by *Advances in Production Engineering & Management* should be submitted by e-mail to the journal Editor-in-Chief:

Miran Brezocnik, Editor-in-Chief
UNIVERSITY OF MARIBOR
Faculty of Mechanical Engineering
Production Engineering Institute
Smetanova ulica 17, SI – 2000 Maribor
Slovenia, European Union
E-mail: editor@apem-journal.org

Manuscript preparation

Manuscript should be prepared in *Microsoft Word 2007* (or higher version) word processor. *Word .docx* format is required. Papers on A4 format, single-spaced, typed in one column, using body text font size of 11 pt, should have between 8 and 12 pages, including abstract, keywords, body text, figures, tables, acknowledgements (if any), references, and appendices (if any). The title of the paper, authors' names, affiliations and headings of the body text should be in *Calibri* font. Body text, figures and tables captions have to be written in *Cambria* font. Mathematical equations and expressions must be set in *Microsoft Word Equation Editor* and written in *Cambria Math* font. For detail instructions on manuscript preparation please see instruction for authors in the *APEM journal* homepage *apem-journal.org*.

The review process

Every manuscript submitted for possible publication in the *APEM journal* is first briefly reviewed by the editor for general suitability for the journal. Notification of successful submission is sent. After initial screening the manuscript is passed on to at least two referees. A double-blind peer review process ensures the content's validity and relevance. Optionally, authors are invited to suggest up to three well-respected experts in the field discussed in the article who might act as reviewers. The review process can take up to eight weeks. Based on the comments of the referees, the editor will take a decision about the paper. The following decisions can be made: accepting the paper, reconsidering the paper after changes, or rejecting the paper. Accepted papers may not be offered elsewhere for publication. The editor may, in some circumstances, vary this process at his discretion.

Proofs

Proofs will be sent to the corresponding author and should be returned within 3 days of receipt. Corrections should be restricted to typesetting errors and minor changes.

Offprints

An e-offprint, i.e., a PDF version of the published article, will be sent by e-mail to the corresponding author. Additionally, one complete copy of the journal will be sent free of charge to the corresponding author of the published article.

APEM
journal

Contents